Laboratory Data on Ices, Refractory Carbonaceous Materials, and Minerals Relevant to Transneptunian Objects and Centaurs

C. de Bergh
LESIA, Observatoire de Paris

B. Schmitt
Laboratoire de Planétologie de Grenoble, CNRS–Université Joseph Fourier

L. V. Moroz
Institut für Planetologie, Universitat Münster, and Institut für Planetenforschung, DLR, Berlin

E. Quirico
Laboratoire de Planétologie de Grenoble, CNRS–Université Joseph Fourier

D. P. Cruikshank
NASA Ames Research Center

Information on the surface compositions of transneptunian objects (TNOs) and Centaurs is derived primarily from spectrophotometric or spectroscopic observations. The identification of the surface constituents and detailed studies of the surface composition depend on the availability of appropriate laboratory data. In particular, optical constants (complex refractive indices) are necessary to calculate synthetic spectra for different grain sizes or deal with components mixed in various ways. Observations of TNOs and Centaurs are made primarily in the wavelength region of reflected sunlight ($0.3 < \lambda < 5$ μm), while some of these objects can be studied in the region of their thermal IR emission ($\lambda > 10$ μm). We review the general spectroscopic characteristics and available optical constants for the ices, refractory carbonaceous materials, and minerals that have been detected or are expected to be present at the surfaces of these objects.

1. INTRODUCTION

Here we review what we know from the laboratory about the surface constituents detected so far at the surfaces of transneptunian objects (TNOs) (Pluto and Charon included) and Centaurs, or that are expected either because they are present in related objects [Triton, irregular satellites of the outer planets, some asteroids, meteorites, comets, and interplanetary dust particles (IDPs)] or because they are easily formed in the laboratory by irradiation or impact of already detected species.

The compounds detected so far with certainty (from well-identified absorption features) at the surfaces of TNOs (including Pluto-Charon) and Centaurs are water ice, methane ice, nitrogen ice, carbon monoxide ice, and ethane ice. In addition, methanol ice (or ice of a photolytic product of methanol) may be present at the surfaces of two objects (absorption feature detected around 2.27 μm). Furthermore, emission features due to fine-grained silicates are detected in thermal-IR spectra of Centaur Asbolus, a signature at 2.2 μm present in spectra of Charon has been tentatively assigned to a mixture of ammonia and ammonia-hydrate, and weak features in visible and near-IR spectra of a few TNOs have been tentatively attributed to hydrated minerals (see chapters by Barucci et al. and Brown).

Additional materials have been introduced in models to account for the general shapes of the spectra, the slopes (or colors) in the visible and near-IR ranges (which are most often different), the possible convexity or concavity of the spectra at the short-wavelength end of the visible spectra, and the (relatively few) measured albedos. These materials include ices, minerals, and complex organic solids (see chapter by Barucci et al.). Since the surfaces are subjected to ultraviolet, solar wind, and cosmic ray irradiation (see chapter by Hudson et al.), irradiated materials have been considered as well as "fresh" materials. The presence of "fresh" materials on TNOs, in spite of continuous exposure to the space environment, could be due to cryovolcanism,

seasonal recondensation of the atmosphere, cometary-type activity, or big impacts. Furthermore, although the dust environment in the region of TNOs is unknown, these objects are thought to be subjected to micrometeoroid impacts that affect the uppermost (and optically visible) regolith by slowly exposing less irradiated material from below the more heavily irradiated crust. The suite of plausible materials with which the models can be calculated is severely limited by the paucity of optical constants available. Prominent among the non-ice materials used in modeling the colors and spectra of TNOs and Centaurs are the so-called Titan or Triton tholins, which are produced in the laboratory by irradiation of gaseous methane-nitrogen mixtures. Also widely used are ice tholins, produced by irradiation of simple hydrocarbon-containing H_2O ices, and kerogen-type material (as an analog of the fine-grained matrix material of carbonaceous chondrites).

In this chapter we review the available optical constants or the spectra covering the visible (0.3 μm < λ < 1.0 μm), near-IR (1 < λ < ~3 μm), mid-IR (~3 μm < λ < 5 μm), and in some cases far-IR (beyond 5 μm), spectral regions for various kinds of detected or plausible TNOs surface materials. The optical constants of a material are the real and imaginary components of the complex refractive index. The refractive index, ñ, of a substance describes the interaction of electromagnetic (EM) radiation with that material. The refractive index is a complex number, consisting of a real and an imaginary component, $\tilde{n} = n + ik$. In this representation, n is the "real" index of refraction, and k is the extinction coefficient, which describes the damping of an EM wave in the material. Both n and k are wavelength dependent. As EM radiation passes through the material, some fraction is absorbed per unit distance it travels, according to the Beer-Lambert law, which allows the calculation of the absorption coefficient α. If λ is the (vacuum) wavelength of the EM radiation of interest, then the imaginary index $k = \lambda\alpha/4\pi$.

We also list or give references to the bands (or type of transitions) that are detected, and note the dependence of the spectra with phase and temperature, grain size, composition (mixtures of ices, etc.) and mode of formation. For each class of materials we examine what laboratory work is needed to make further progress in the study of the surfaces of TNOs and Centaurs. For the irradiation experiments required, we refer to the chapter by Hudson et al.

2. REQUIRED LABORATORY DATA

The identification of the materials present at the surface of TNOs requires the knowledge of the spectral properties of these materials over the UV, visible, and IR ranges. Indeed, the only current means of observation of these surfaces is by optical and IR remote sensing (photometry, spectroscopy, and imagery, but also imaging spectroscopy for the New Horizons mission) either from groundbased telescopes or from space.

The first goal of remote sensing is to detect and identify the materials present at the surface, derive some information on the ways they are mixed (at molecular, granular, or geographic and stratigraphic levels), and estimate their relative abundances. Various physical and thermodynamic properties such as temperature, thermal history, the state of the ices (crystalline, amorphous) and the texture of the surface (grain size, surface compactness, roughness) may also be inferred by using some specific spectral or photometric tracers. In order to retrieve all this information from surface spectra, either in reflectance or in emission, laboratory data of relevant materials (ices, solid organics, carbonaceous materials, minerals) in conditions appropriate for TNOs are absolutely required. In addition, optical constants are calculated from laboratory spectra to estimate reflectance and emittance of particulate surfaces by radiative transfer models. The quality of the laboratory data and models should be commensurate with the quality of the observational data in order not to limit their interpretation.

The photon flux coming from a surface has two components: reflected solar radiation and thermal emission by the surface, with relative intensities depending on the wavelength considered. Because of the very low temperatures of TNO surfaces (~20 K < T < 60 K), the transition between the solar reflection and thermal emission regimes occurs at long wavelength, typically at λ > 20–30 μm. Thus reflectance spectra in the region normally accessible for TNOs (wavelengths less than about 5 μm) are not perturbed by thermal emission and therefore give access to part (2.5–5 μm) of the range of the fundamental vibrations of most molecules. Although these very strong bands are frequently saturated in reflectance spectra, they add interesting constraints on the surface composition when analyzed together with the better defined combination and overtone bands controlling the near-IR spectrum. The visible range also contains some spectral information (mostly the wing of strong UV bands with possible structures, some weak CH_4 bands, etc.) but, as discussed later, the constraints they add on specific phases (organics, carbonaceous materials, minerals) in terms of surface composition are not always strong. At the other end of the spectrum the thermal emission dominates the far-IR range (>20–30 μm), but extracting information from emission spectra is more complicated due to a lack of accurate emission radiative transfer models within surfaces and of appropriate laboratory emission spectra of relevant materials.

Direct comparison of a TNO spectrum with laboratory transmission or reflectance spectra may be enough to identify the main components of a surface and to have some first idea of its physical state. Laboratory reflectance spectra can be linearly combined to simulate, as a first approach, a geographic (or spatial) mixture of materials, but this approach is very limited in terms of surface description. Most of the spectral data on minerals are available as reflectance spectra. While for ices only few laboratory reflectance spectra are available, it is possible to calculate these reflectance

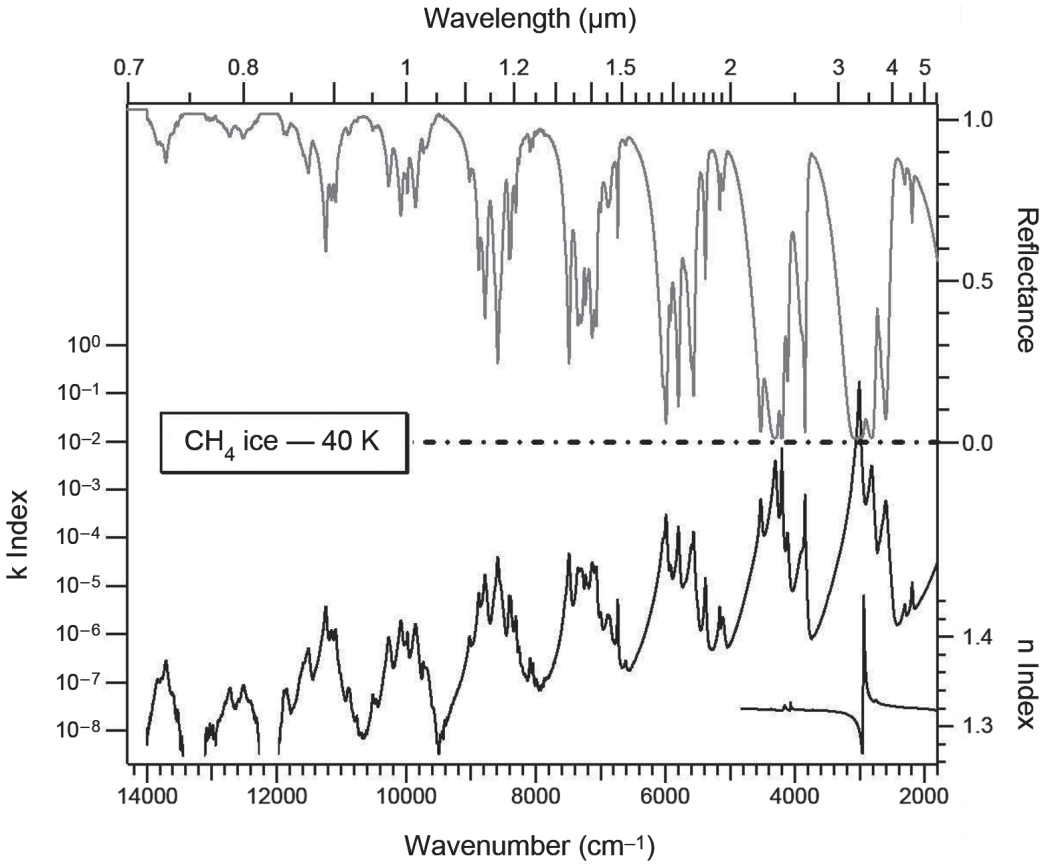

Fig. 1. *Lower curves*: Optical constant (k, n) spectra of CH_4 ice at 40 K in the visible, near-IR, and mid-IR (*Grundy et al.,* 2002; *Schmitt et al.,* 1998). The n index below 2 μm (>5000 cm^{-1}), not shown on the figure, decreases linearly from 1.36 at 15,800 cm^{-1} (0.63 μm) to 1.32 at 5000 cm^{-1} (2 μm). The data have been compiled using six experiments with thicknesses varying from a few micrometers (thin films deposited from the gas phase) to 1 cm (crystal grown from liquid in a closed cell). *Upper curve*: Reflectance spectrum of a CH_4 ice surface with 500-μm grain size, calculated from the optical constants.

spectra in cases where the complex refractive indices have been determined (which requires transmission spectra). Reflectance spectra have also been obtained for a limited number of relevant mixtures of ices with organics and minerals. We note, however, that the physical state of the laboratory samples is often not relevant for TNOs in terms of temperature, phase, grain size, etc. In particular, the samples measured in reflectance are typically at temperatures of 77 K or above.

The determination of the state of mixing, composition, and texture of the surface materials, as well as the extraction and identification of faint signatures, require detailed radiative transfer modeling. Such modeling requires the optical constants of the materials to simulate the reflectance spectrum of the surface, but also some frequently unknown parameters such as the single-scattering phase function of the medium (see chapter by Barucci et al.). However, measuring the optical constants is not a simple matter. In particular, for the major ices of interest here, the variation of the absorption coefficient in the entire visible, near-IR, and mid-IR ranges covers several orders of magnitude (e.g., Fig. 1). A large suite of experiments with various sample thicknesses and measurement techniques is therefore needed to obtain the spectral transmission measurements required to compile an optical constant spectrum over a wide spectral range, for example from 0.8 to 5 μm. Approximate optical constants can, however, be extracted from reflectance measurements (*Hapke and Wells,* 1981; *Clark and Roush,* 1984; *Shkuratov et al.,* 1999; *Roush,* 2003). For materials only available as powders (most minerals and organics) this technique, which requires several assumptions, currently provides the only available option to enable the inclusion of these materials in radiative transfer models. However, these data need to be used with care, especially when considering their absolute values (*Douté et al.,* 2007).

In our review, we will not focus on detailed description of the slopes and shapes of reflectance spectra. Direct comparisons between the spectra of TNOs/Centaurs and their analogue materials in terms of slopes and shapes may be misleading. For many relevant phases, visible and near-IR

(VNIR) spectral slopes strongly depend on grain size and composition within a given class of material (e.g., tholins, kerogens). In addition, a dark material (e.g., amorphous carbon) may be spectrally neutral as a pure particulate phase but may induce spectral reddening if the dark material is fine-grained and intimately mixed with a bright phase (ice or mineral) or forms a thin film or dust layer on a bright phase. Similar effects can alter the spectral shapes. For example, VNIR spectra of pure coals and bitumens are concave due to a broad saturated UV absorption. However, the spectral curves may become convex for intimate mixtures with bright phases, especially if those bright phases have convex visible spectra (e.g., Fe-bearing silicates). The application of an appropriate spectral mixing model may help to establish the presence or absence of a certain phase on the surface of a TNO or Centaur.

In the following, we will review the optical constants available (or spectra when the constants are missing) in the spectral ranges relevant to current observations of TNOs, with particular emphasis on the visible and near-IR (0.3–5 μm).

3. ICES

Many laboratory spectra of ices have been recorded in the mid- and far-IR ranges ($\lambda > 2.5$ μm) at low temperatures, mostly for purely spectroscopic aims but also for the study of icy mantles condensed on dust grains in the interstellar medium (ISM). However, the ices of TNOs have compositions, physical states (phase, temperature, etc.), and thermal histories radically different from the ISM grains. Nevertheless, some of these data are useful in analyzing the fundamental bands of ices in the 3–5-μm region and will be briefly reviewed in this chapter. Note, however, that because of details of the radiative transfer, these strong bands are frequently saturated in reflectance spectra of surfaces, contrary to spectra of grains in the ISM.

The analysis of the near-IR spectra of the icy objects Triton and Pluto has already triggered several in-depth laboratory spectral studies of ices encompassing their specific physico-chemical conditions, and therefore also appropriate for TNOs (see sections 3.2–3.5). In particular, *Quirico and Schmitt* (1997a) studied the spectra of methane ice and methane diluted in nitrogen by growing crystals in a closed cell from the liquid phase, finding that these long pathlength samples grown under thermodynamical equilibrium are particularly appropriate for the surfaces of Triton and Pluto. These two similar bodies appear to have large surface exposures of polycrystalline N_2 in which small amounts of CH_4, CO, and perhaps other molecules are dissolved in vapor-pressure equilibrium with the tenuous atmospheres. Due to their complexity, these experiments are currently quite limited. However, thin films experiments with some volatile ices condensed from the gas phase can provide useful transmission spectra, particularly on the strongest near-IR bands, as long as the condensation conditions (and temperature) of the sample, and thus its physical state, are representative of the object studied. In any case, optical constants in both the visible and near-IR spectral ranges and at appropriate physical conditions for these cold objects are still seriously lacking for several important molecules or mixtures.

Many TNOs and Centaurs are covered, at least partly, by ices of low volatility, such as H_2O, that may be out of thermodynamic equilibrium (in terms of phase, for example) due to the low surface temperatures (~20–60 K) or to endogenic/exogenic processes (particle bombardment, impact gardening, etc.). Laboratory experiments should then consider these possibilities (see also chapter by Hudson et al.), as well as the effects of thermal history of the surface on the spectra. Most of these laboratory studies have been performed in the mid-IR with vapor-deposited samples.

The relevance of different types of laboratory measurements for ices (transmission through thin films and crystals, diffuse reflection in various geometries, etc.) to the study of solar system objects, as well as the methods for extracting the optical constants, have been discussed in some detail in a few books and papers (e.g., *Schmitt et al.,* 1998) and will not be repeated here, except when necessary. A detailed discussion of the effects of the various physical parameters that affect the spectra of ices and their mixtures is also available in *Schmitt et al.* (1998) and *Brown and Cruikshank* (1997).

In the following we will briefly review the available optical constants (or absorption coefficient, or spectra if only they are available) of the different (pure and mixed) ices of interest for TNO surface spectral analysis.

3.1. Water Ice

In addition to its presence on satellites of Jupiter, Saturn, and Uranus, water ice is found on Triton, Pluto (tentative), and seems to dominate the surface of Charon and many TNOs and Centaurs. Water ice shows about ten crystalline forms, with only two or three that are stable at low pressure (a cubic Ic, an hexagonal Ih, and possibly an orthorhombic ice XI), three amorphous forms (Ia), and a glassy phase.

Because water ice is one of the most widespread materials in the solar system, many authors have studied its optical properties through transmission and reflectance spectroscopy. Many of these studies were made with emphasis on the effects of temperature, phase, and thermal history on specific IR bands (e.g. *Schmitt et al.,* 1989; *Moore and Hudson,* 1992; *Smith et al.*, 1994). The most recent review, although partly updated, of the available spectra and optical constants of crystalline ice from the UV to the far-IR has been made by *Warren* (1984). All references prior to 1982 can be found in that paper. However, most of the data used for the calculation of the optical constants have been recorded at fairly high temperatures (between 80 and 263 K) and are thus not fully relevant for TNO studies.

More recently, a consistent set of absorption coefficients of crystalline water ice has been determined in the near IR (from 1 to 2.7 μm) at many different temperatures between 20 and 270 K (*Grundy and Schmitt,* 1998). In this dataset only the interband absorption near 1.1 μm has a substantial uncertainty. The spectral changes with temperatures were analyzed and the temperature-dependent spectrum was resolved as a set of 15 overlapping Gaussian curves with band parameters allowing synthesizing of the optical constants of crystalline water ice at any temperature.

Fink and Sill (1982) published the first near-IR transmission spectra of the amorphous phase of H_2O at different temperatures. *Schmitt et al.* (1998) also determined absorption coefficient spectra at 40 K and 140 K that have been used in several spectral models (e.g., *Cruikshank et al.,* 2000). Near-IR spectra at 10 K (*Gerakines et al.,* 2005) and between 40 and 125 K (*Mastrapa and Brown,* 2006) have also been recorded recently. However, due to the difficulty in obtaining thick amorphous samples these data are incomplete (no data below 1.4 μm).

In the mid-IR a dozen papers have concerned the calculation of the optical constants of water ice at low temperature (10–190 K) in its amorphous and crystalline forms (see *Warren,* 1984; *Hudgins et al.,* 1993; *Toon et al.,* 1994; *Trotta,* 1996; *Schmitt et al.,* 1998). There are significant differences in the indices calculated by various authors, mainly due to improved experimental techniques and optical constant extraction codes (for recent comparisons, see *Toon et al.,* 1994; *Trotta,* 1996).

Water ice may be mixed with some other ices on TNO surfaces. Many studies have been performed for the fundamental bands of water mixed or diluted in a large variety of other ices but only very limited data have been reported in the near-IR and only for the strongest water bands in N_2 ice (*Palumbo and Strazzulla,* 2003; *Satorre et al.,* 2001). The principal effect is that the broad water ice bands transform into narrow bands strongly shifted in wavelength.

3.2. Nitrogen Ice

Solid nitrogen exhibits two phases: below 35.6 K, the cubic α phase is stable; above this temperature it is the field of the hexagonal β phase. This last phase seems to be dominant on Pluto and Triton, and may be present on TNOs 90377 Sedna and 136199 Eris (formerly 2003 UB_{313}). On some TNOs with lower surface temperatures α-nitrogen may exist.

Very weak IR bands have been observed for both crystalline phases in the near-IR (first overtone region) (*Schmitt et al.,* 1990; *Green et al.,* 1991) and in the mid-IR (fundamental stretching vibration range) (*Tryka et al.,* 1995; *Quirico et al.,* 1996). Detailed studies and absorption coefficient spectra of both phases at various temperatures between 20 and 63 K were published (*Grundy et al.,* 1993; *Tryka et al.,* 1993, 1995; *Schmitt et al.,* 1998). The α phase displays very narrow absorptions, the main ones peaking at 2.148 μm and in the 4.15–4.30-μm range, requiring high spectral resolution for detection, while the β phase has broad bands around 2.15, 4.18, and 4.29 μm. The transition and possibly the spectral shape of the bands can be used as a surface thermometer (*Grundy et al.,* 1993).

When other molecules, especially CO_2 and H_2O, are dissolved in nitrogen ice, a very strong enhancement in the band strength of the N_2 absorption occurs. But this effect has been studied only for the fundamental vibration band of α-nitrogen (e.g., *Nelander,* 1976; *Bernstein and Sandford,* 1999).

3.3. Methane Ice

Methane ice has been found on Pluto and Triton either in pure form (on Pluto) or diluted in nitrogen (on both bodies). It is also observed on the TNOs 2005 FY_9 and Eris (2003 UB_{313}). Solid methane presents two phases: the cubic phase II below 20.4 K and the cubic phase I above.

Several near-IR reflectance (see, e.g., *Fink and Sill,* 1982) and transmission spectra (e.g., *Schmitt et al.,* 1992) have been published, but the first optical constants for CH_4 ice in both phases (at 10 K and 33 K) are from *Khare et al.* (1990a) and *Pearl et al.* (1991). *Quirico and Schmitt* (1997a) published a high-resolution near-IR absorption coefficient spectrum of phase I at 21 K. Complete absorption coefficient spectra covering the 0.7–5-μm range for various temperatures between 15 and 90 K were obtained for both phases of pure methane by *Grundy et al.* (2002). They also studied the use of some bands, especially in the region around 2.55–2.6 μm, as a thermometer for pure CH_4 frost. The spectrum at 40 K is shown in Fig. 1.

Several spectroscopic studies were performed in the mid-IR range (see review by *Quirico and Schmitt,* 1997a) and a few sets of optical constants of solid CH_4 are available for both phases between 10 and 30 K (*Pearl et al.,* 1991; *Hudgins et al.,* 1993; *Trotta,* 1996). Optical constants at higher temperatures (i.e., 38 K) have been published by *Schmitt et al.* (1998).

Spectra of methane diluted at low concentration in solid nitrogen have been studied by *Quirico and Schmitt* (1997a). They derived normalized absorption coefficients at different temperatures in both nitrogen ice phases that were used to simulate the spectra of Triton and Pluto (*Quirico et al.,* 1999; *Douté et al.,* 1999; *Cruikshank et al.,* 2000). The spectra were derived from transmission measurements through monocrystalline samples grown in closed cells. However, from the modeling of Triton and Pluto spectra it has been found that the existing spectral data for diluted methane are not yet sufficient to model the regions of weak absorptions between the strong methane bands. This problem may be even more crucial for some TNOs that have methane absorptions substantially stronger than those of Pluto, although if there is no N_2 the appropriate data are those for pure CH_4. The near-IR spectrum of methane-water ice mixtures has also been studied (*Bernstein et al.,* 2006); slight shifts in

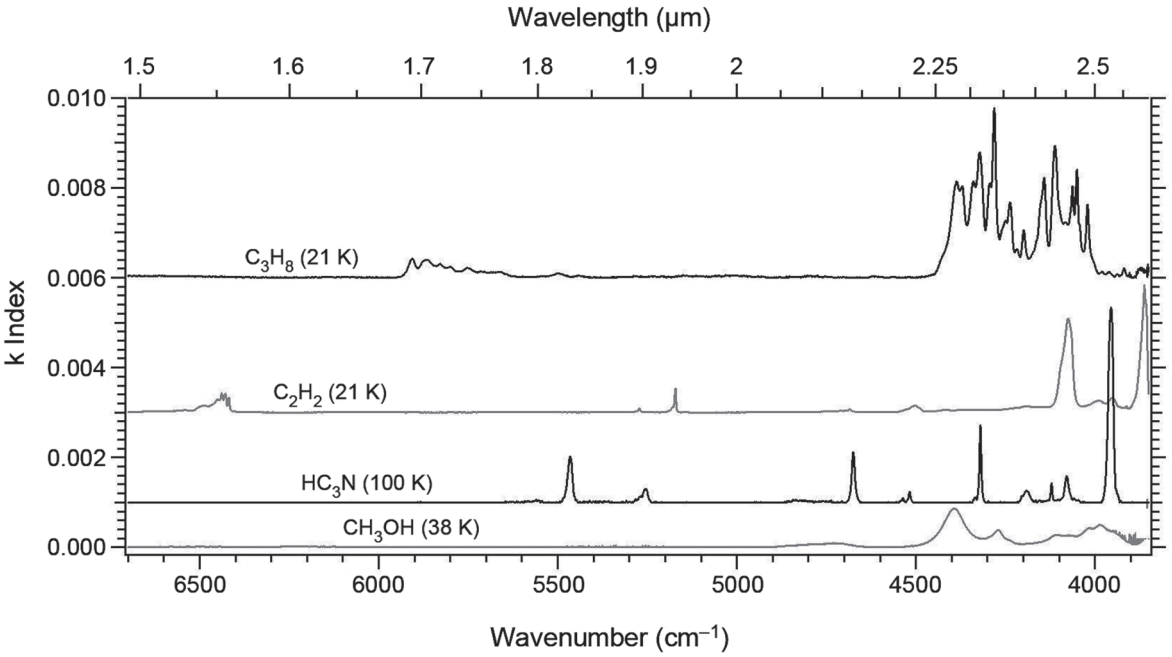

Fig. 2. Near-IR imaginary index (k) spectra of C_2H_2 (21 K), C_3H_8 (21K), HC_3N (100 K), and CH_3OH (38K) ices [derived from transmission spectra acquired at LPG and published in *Quirico et al.* (1999)]. The n index cannot be derived from these experiments.

band positions and significant band broadenings are observed.

3.4. Other Simple Solid Hydrocarbons

Light hydrocarbons can be efficiently produced by low-temperature irradiation of methane (see chapter by Hudson et al.). Although only ethane ice has been (tentatively) detected on the surface of Pluto so far, other simple, and possibly some large, hydrocarbons could be present as well, and are indeed predicted by photochemical models of Pluto's atmosphere (e.g., *Krasnopolsky and Cruikshank,* 1999).

3.4.1. Acetylene (C_2H_2). Acetylene presents a single solid-phase transition at 133 K. Only a few spectral studies have been devoted to solid acetylene, including a single set of mid-IR optical constants at 40 K (*Khanna et al.,* 1988) and a single near-IR spectrum at about 20 K (*Quirico et al.,* 1999). We show the corresponding imaginary index of the optical constants in Fig. 2.

3.4.2. Ethylene (C_2H_4). For ethylene, two phase transitions, one below 20 K and another near 50 K, are suspected. Near-IR measurements were performed by *Schmitt et al.* (1992), and *Quirico and Schmitt* (1997a) published absorption coefficients at 21 K. The effects of dilution at low concentration (1%) in nitrogen ice have also been studied by these authors. Although the mid-IR spectrum of ethylene has been extensively studied at many temperatures up to 93 K (see review by *Quirico and Schmitt,* 1997a), only a single set of optical constants (at 15 K) has been calculated so far (*Trotta,* 1996).

3.4.3. Ethane (C_2H_6). At low temperature ethane presents an amorphous phase below 25 K, a metastable phase between 25 and 60 K, and two crystalline phases (transition at 88.9 K). The optical constants of ethane at 30 K computed over part of the near-IR range by *Pearl et al.* (1991) have been completed by *Quirico and Schmitt* (1997a) from transmission spectra at 21 K (*Schmitt et al.,* 1992). These authors also recorded the spectrum of this molecule diluted at low concentration (1%) in nitrogen ice. The spectra of the different phases of solid C_2H_6 were recorded in the mid-IR range (see *Wisnosky et al.,* 1983) but the optical constants calculated at 15 and 30 K in this spectral range (*Trotta,* 1996; *Pearl et al.,* 1991) only concern the crystalline phase II.

3.4.4. Larger hydrocarbons. Hydrocarbons with three or more carbon atoms have been studied almost exclusively in the mid-IR where a few spectra are available at low temperature, especially for alkanes (e.g., *Goodman et al.,* 1983, *d'Hendecourt and Allamandola,* 1986). Optical constants have been published only for solid C_4H_2 at 70 K (*Khanna et al.,* 1988). *Bohn et al.* (1994) studied the mid-IR and part of the near-IR spectra (above 2 μm) of a series of large hydrocarbon molecules (up to C_8H_{18}) diluted in α-N_2 at very low temperature while *Quirico et al.* (1999) presented a first near-IR spectrum of solid propane (C_3H_8) at 21 K. We show the corresponding imaginary index of the optical constants in Fig. 2.

Curchin et al. (2006 and in preparation) have obtained reflectance spectra of a large number of hydrocarbons and other organic compounds in the solid phase, recorded at temperatures ~80–90 K, in the wavelength range 0.35–15.5 μm.

Their samples include alkanes, cycloalkanes, alkenes, alkynes, aromatics, nitriles, amines, and cyanides.

3.5. Carbon Monoxide and Carbon Dioxide Ices

Solid CO was observed on Triton and Pluto, while solid CO_2 was detected on Triton, Ariel, Umbriel, and Titania (for other outer planet satellites, the detected CO_2 is either trapped or complexed with other materials).

3.5.1. Carbon monoxide (CO). Solid carbon monoxide exibits a phase transition at 61.6 K; the low temperature α-phase is cubic and the high temperature β-phase is hexagonal.

The two overtone bands in the near-IR (1.577 and 2.404 μm) were first measured in transmission (see *Fink and Sill,* 1982; and review in *Quirico and Schmitt,* 1997a). The only published absorption coefficient spectrum of CO ice (at 20 K), with isotopic band assignments, can be found in *Quirico and Schmitt* (1997a) who also studied the spectra of CO diluted in the two phases of nitrogen ice at different temperatures (*Quirico and Schmitt,* 1997b). The fundamental region (around 4.68 μm) in the mid-IR has been studied by several authors but optical constants are only available at very low temperatures (10–15 K) (*Hudgins et al.,* 1993; *Trotta,* 1996).

3.5.2. Carbon dioxide (CO_2). Solid carbon dioxide has only one crystalline phase (cubic) at zero pressure, but amorphous and glassy CO_2 can form below 10–30 K. *Warren* (1986) reviewed all the available spectroscopic measurements on CO_2 ice and computed optical constants from the UV to the microwave region.

Reflectance spectra of this molecule in the near-IR have been recorded several times but only a few transmission spectra are available (*Schmitt et al.,* 1994; *Hansen,* 1996; *Bernstein et al.,* 2005). Absorption coefficients for the four strongest near-IR bands were estimated by *Warren* (1986) from data of *Fink and Sill* (1982) and completed by *Calvin* (1990) from reflectance measurements. High-spectral-resolution data for CO_2 ice have now been published (*Quirico and Schmitt,* 1997a). The weakest near-IR bands and the interband continuum absorption of CO_2 ice have been also measured in detail at 150 K by *Hansen* (1997, 2005) over a wide spectral range.

Several transmission studies of CO_2 ice have been performed in the mid-IR, and optical constants are given in those wavelength regions at a few temperatures between 10 and 160 K (*Warren,* 1986; *Hudgins et al.,* 1993; *Hansen,* 1997; *Trotta,* 1996; *Schmitt et al.,* 1998). Large differences exist among these different sets (see *Trotta,* 1996), mainly due to the extraction method.

The mid- and near-IR spectra of CO_2 diluted in various solids have been studied. Of relevance to TNOs are the studies in nitrogen ice (*Quirico and Schmitt*, 1997a) and in water and methanol ices (*Bernstein et al.,* 2005). Dilution permits the appearance of a new overtone band (inactive in pure CO_2) around 2.134 μm. This band is a potential indicator of the state of mixing of the CO_2.

3.6. Solid Ammonia and Ammonia-Hydrates

Ammonia ices have always been considered as a likely component of icy outer solar system satellites, helping to explain their complex geological histories. An absorption feature observed at 2.2 μm in the spectrum of Charon is probably a combination of ammonia and ammonia-hydrate.

Ammonia ice presents only one stable cubic crystalline phase, but an amorphous or glassy phase (below 60–80 K) and an intermediate, metastable phase (below 100–120 K) have been also observed.

After a first review of the spectroscopic measurements on NH_3 ice by *Taylor* (1973) and derivation of its optical constants in the IR, a more detailed study by *Martonchik et al.* (1984) covered the near-UV to the far-IR.

In the near-IR, a few reflectance spectra at low temperatures (77–150 K) have been published (e.g., *Fink and Sill,* 1982), as well as an absorption coefficient spectrum (down to 1.5 μm) of the cubic phase at 88 K (*Sill et al.,* 1980) used to calculate its optical constants (*Martonchick et al.,* 1984). Absorption coefficients over part of the near-IR for the metastable (40 K) and the cubic phases (70 K) of NH_3 ice between 1.8 and 2.5 μm were published by *Quirico et al.* (1999) and *Schmitt et al.* (1998). A partial spectrum of amorphous NH_3 at 10 K is also available (*Gerakines et al.,* 2005).

In addition to many spectroscopic studies of NH_3 ice in its various phases in the mid-IR, absorption coefficients of the crystalline phase are available in both ranges (*Sill et al.,* 1980) and optical constants have been calculated at various temperatures between 15 and 195 K (*Martonchik et al.,* 1984; *Mukai and Krätschmer,* 1986; *Trotta and Schmitt,* 1996).

There are at least three types of ammonia hydrates known to exist at low pressure: the hemihydrate ($2NH_3.H_2O$), the monohydrate ($NH_3.H_2O$, or NH_4OH), and the dihydrate ($NH_3.2H_2O$). Amorphous structures also exist at low temperature and NH_3 may also occur as a solid solution in water ice, in particular at low concentration. A series of studies has been conducted in the mid-IR to analyze spectra of these hydrates at 100 K (*Bertie and Shehata,* 1984, 1985; *Bertie and Devlin,* 1984). The hemihydrate, also studied at lower temperatures, shows two crystalline phases with a transition at 52 K (*Bertie and Devlin,* 1984).

In the near-IR a single set of reflectance spectra of ammonia-water mixtures at 77 K with four different concentrations (1–30%) is shown in one of the figures in *Brown et al.* (1988), and *Cruikshank et al.* (2005a) summarized their near-IR band positions. Clear spectral shifts (to shorter wavelengths for the 2.0- and 2.24-μm bands) and relative intensities changes occur upon hydration of ammonia (*Schmitt et al.,* 1998). Recently *Moore et al.* (2007) performed low-temperature (10–165 K) near- and mid-IR spectroscopic studies (1.8 to 20 μm) of ammonia ice and water-ammonia mixtures with special emphasis on features in the near-IR, but no absorption coefficients are derived. Spectral shifts of the bands toward higher wavenumbers occur upon dilution of NH_3, but in the near-IR no clear spectral differences

are observed between the stoichiometric hydrates and icy mixtures with identical NH_3 concentrations.

3.7. Nitriles Ices

Simple nitriles, such as found in cometary comae, could be present as ices at the surface of TNOs (see chapter by Hudson et al.).

3.7.1. Hydrogen cyanide (HCN). Hydrogen cyanide has an orthorhombic low-temperature phase (<170 K). To the best of our knowledge, no spectra are available in the UV to near-IR range. Spectra of HCN polymer recorded at room temperature (*Cruikshank et al.,* 1991) are sometimes used in models instead.

Mid- and far-IR spectra have been recorded for the low-temperature phase of HCN between 35 and 95 K (see *Masterson and Khanna,* 1990; *Dello Russo and Khanna,* 1996) and optical constants were published in the mid-IR at 60 K (*Masterson and Khanna,* 1990). HCN polymers have also been studied from the UV to the mid-IR and optical constants have been calculated (see *Khare et al.,* 1994) (see also section 4.2).

3.7.2. Larger nitriles. The mid-IR transmission spectra of several larger solid nitriles have been studied at low temperatures (<100 K). *Dello Russo and Khanna* (1996) recorded the spectra at 35 K and 95 K of cyanogen (C_2N_2), dicyanoacetylene (C_4N_2), acetonitrile (CH_3CN), cyanoacetylene (HC_3N), cyanopropyne (CH_3C_3N), acrylonitrile (CH_2CHCN), and propionitrile (CH_3CH_2CN). They also systematically gave the integrated band intensities, and optical constants in the main bands above 12 μm. Mid-IR optical constants have been also published by other authors for C_2N_2 at 20 K (*Ospina et al.,* 1988), as well as for C_4N_2 and HC_3N at 60 K (*Masterson and Khanna,* 1990). The IR spectrum of CH_3CN has been studied by several authors (e.g., *d'Hendecourt and Allamandola,* 1986).

In the near-IR, absorption coefficients are available only for HC_3N (*Quirico et al.,* 1999). We present the corresponding imaginary index of the optical constants in Fig. 2.

Cruikshank et al. (1998) published a room-temperature reflectance spectrum of piperazine ($NHCH_2CH_2NHCH_2CH_2$), an amine similar in structure to trioxane [the formaldehyde trimer $(HCHO)_3$], 0.3–2.5 μm. They also published a reflectance spectrum in the same region of hexamethylenetetramine [$(CH_2)_6N_4$], a molecule of interest because it carries four atoms of N and its synthesis incorporates NH_3.

3.8. Methanol and Formaldehyde Ices

Methanol ice is probably present at the surface of Centaur Pholus and one TNO. Formaldehyde, detected in cometary comae, is another plausible icy surface component for TNOs.

Solid methanol has two hydrogen bonded crystalline phases with a transition at 157 K, and an amorphous phase below 78 K. A few spectra of methanol ice are available over part of the near-IR (*Cruikshank et al.,* 1998; *Quirico et al.,* 1999; *Brunetto et al.,* 2005, *Bernstein et al.,* 2005), but its spectrum is unknown below 2 μm. Figure 2 displays the imaginary index of the optical constants of CH_3OH at 38 K derived from *Quirico et al.* (1999).

On the other hand, there are numerous studies available for the mid- and far-IR transmission spectra of solid CH_3OH and its isotopic species (e.g., *d'Hendecourt and Allamandola,* 1986; *Hudson and Moore,* 1993; *Moore et al.,* 1994), and optical constants have been calculated between 10 and 120 K (*Hudgins et al.,* 1993; *Trotta,* 1996).

Formaldehyde (H_2CO) has been less studied, and essentially in the mid-IR range (e.g., *Harvey and Ogilvie,* 1962), but with no optical constants available as a pure solid. The only data published in the visible and near-IR (0.3–2.5 μm) are that of the paraformaldehyde polymer (*Cruikshank et al.,* 1998). Of relevance for TNOs, part of the near-IR spectrum (>2 μm) of formaldehyde molecules highly diluted in α-N_2 ice was also published by *Bohn et al.* (1994).

3.9. What is Missing

A number of laboratory studies have already recorded the spectra and derived the optical constants of several pure ices (H_2O, CH_4, N_2, CO, etc.) in many different physical conditions (temperature, phase, mixing). However, there are still several molecules that either have been studied only at temperatures irrelevant to TNOs or are available mostly as reflectance spectra. In other cases, the available transmission spectra incompletely cover the near-IR range. In particular, the molecules with incomplete data below 2 μm include NH_3, CH_3OH, C_2H_2, C_2H_4, C_3H_8, HC_3N, and numerous hydrocarbons. For a few others there are still no near-IR spectra available: HCN, H_2CO, all large hydrocarbons ($C \geq 3$, except C_3H_8), and most nitriles. Even when the transmission spectra have been measured, the absorption coefficients or the optical constants (needed for radiative transfer modeling) are not always derived. We note that, as mentioned in section 3.4.4, *Curchin et al.* (2006) have obtained reflectance spectra for a large suite of solid organics and nitriles that will soon become available.

When considering the potential mixtures that may occur on TNOs we can see that the near-IR spectra of many molecules have not yet been recorded in mixtures with the ices suspected to dominate at least part of their surfaces: H_2O, CO_2, β-N_2, CH_4. When data are available, in most cases only the strongest combination/overtone bands are recorded. In the case of the important CH_4-N_2 mixture, only few data have been recorded for mixtures with high concentrations of methane (*Quirico et al.,* 1996). Furthermore, wavelength regions where the absorption is very weak (defining the "continuum") in spectra of some CH_4 and N_2-rich TNOs need to be more accurately measured, as there are remaining and persistent difficulties in fitting these spectral regions with models.

Although significant progress has recently been achieved in understanding the spectra of different phases and types of mixtures of ammonia hydrate (*Moore et al.,* 2007), optical constants still must be measured for the amorphous phase, solid solutions, hemi-, mono-, dihydrates, etc.

Finally, several other species that may be formed by energetic processing of the TNO surface ices, such as H_2O_2, NO, NO_2, N_2O, C_2H_5OH, HCOOH, H_2CO_3, etc., or even cyanate (OCN^-) and ammonium ions (NH_4^+), clearly deserve further studies to extract their optical properties. Their formation and available spectral properties, not dealt with in this chapter, are described in the chapter by Hudson et al.

4. REFRACTORY CARBONACEOUS MATERIALS

Non-icy carbonaceous species of abiotic origin, ranging from very complex hydrocarbon macromolecular materials to pure elemental carbon solids (e.g., graphite, nanodiamonds), are present in primitive meteorites, IDPs, comets, asteroids, and interstellar and circumstellar dust (e.g., *Hayatsu and Anders,* 1981; *Kissel and Krueger,* 1987; *Kerridge,* 1999; *Sandford,* 1996; *Tielens,* 1997; *Pendleton and Allamandola,* 2002; *Huss et al.,* 2003; *Flynn et al.,* 2003; *Quirico et al.,* 2005; *Lisse et al.,* 2006; *Sandford et al.,* 2006). Such carbonaceous species usually have low visual albedos and a wide variety of colors in the visible and near-IR (VNIR) spectral region, ranging from red to neutral. In general, their colors become less red with increasing abundance and size of aromatic moieties in macromolecular material compared to the abundance of H-rich aliphatic chains and/or O-, N-functionalities. Complex hydrocarbon materials often show no absorption features in the VNIR spectral range. Many TNOs and Centaurs have low albedos and show a wide range of VNIR surface colors. This variety in surface optical properties may be (but is not necessarily) controlled by content, composition, and particle sizes of carbonaceous species. Therefore, it is important to acquire optical data on plausible carbonaceous analogs for use in spectral models of TNOs and Centaurs. Complex organics on TNOs and Centaurs may be indigenous, analogous to materials described in section 4.1, and/or may be products of irradiation of surface ices (see sections 4.2 and 4.3). In the absence of optical constants for other potentially useful organic analog materials, tholins are primarily used in models to reproduce red colors of TNOs and Centaurs, while elemental carbon of various kinds (ranging from structurally ordered graphite to amorphous C) is used to reproduce their low albedos.

4.1. Extraterrestrial and Terrestrial Carbonaceous Materials

Extraterrestrial organic materials available for laboratory studies are found in meteorites and IDPs. Over 650 individual organic molecules have been identified in primitive meteorites, but the largest portion (≥90 wt.%) of meteoritic organic matter is represented by a complex macromolecular material insoluble in organic solvents and analogous to kerogen from terrestrial sedimentary rocks (*Durand,* 1980). Meteoritic "kerogens," often referred to as "IOM" (insoluble organic matter), are rich in polycyclic aromatic hydrocarbons.

Since primitive meteorites contain only up to a few weight percent of carbonaceous matter intimately mixed with minerals, a meteorite should be treated with acids to isolate organics for spectral/optical measurements. The acid treatment should be preceded by toluene/methanol extraction of soluble organics to avoid their reaction with acids, making it impossible to separate bulk meteoritic organic matter (insoluble plus soluble fractions) from minerals without its partial loss/damage (e.g., *Robert and Epstein,* 1982; *Halbout et al.,* 1990; *Wright et al.,* 1990; *Kerridge,* 1999). Therefore it must be borne in mind that the acid residues may be optically different from the bulk meteoritic organic matter in case of meteorites containing non-negligible soluble organic fraction, such as CI1 and CM2 chondrites. The careful use of appropriate soft demineralization procedures (e.g., *Cody et al.,* 2002) can minimize the damage to, at least, the insoluble (kerogen-like) fraction.

The optical constants (n, k) of insoluble organic residues from CM2 chondrite Murchison between 0.15 and 40 μm have been published by *Khare et al.* (1990b) and reflectance spectra from 0.2 to 6.5 μm by *Cruikshank et al.* (2001). *Hayatsu et al.* (1977) published transmittance spectra of Murchison IOM from 2.5 to 17 μm and *Flynn et al.* (2004) from 5 to 14 μm. Absorption spectra of the Murchison acid residue in the 3.4-μm spectral region have been published by *Pendleton* (1995) and *Flynn et al.* (2004), and by *Gardinier et al.* (2000) between 2.5 and 25 μm. Infrared transmittance spectra of acid residue from Orgueil (CI1) meteorite have been acquired by *Wdowiak et al.* (1988) (2.5–25 μm), *Ehrenfreund et al.* (1991) (2.5–25 μm), *Gardinier et al.* (2000) (2.5–25 μm), *Brownlee et al.* (2000) (3.2–3.7 μm), and *Flynn et al.* (2004) (5–14 μm). *Murae et al.* (1990) and *Murae* (1994) obtained IR spectra (2.5–25 μm) of carbonaceous insoluble residues from meteorites ALH 77307 and Y 791717 (CO3) and Allende (CV3).

Meteoritic IOM appears to be extremely diverse in composition (e.g., *Alexander et al.,* 1998; *Gardinier et al.,* 2000; *Cody and Alexander,* 2005). Composition and structure of IOM from meteorites of petrologic types higher than 2 (e.g., anhydrous CO3 and CV3 carbonaceous chondrites, ordinary chondrites) are controlled mostly by thermal metamorphism, although there is a debate regarding the heating of IOM on parent bodies vs. solar nebula (e.g., *Alexander et al.,* 1988; *Quirico et al.,* 2003; *Huss et al.,* 2003; *Bonal et al.,* 2006). Such IOM is highly carbonized compared to IOM from hydrated CR2, CI1, CM2 chondrites, and Tagish Lake (C2 ungrouped). Significant compositional and structural diversity exists also between organics from the hydrated meteorites, and it is unclear to what extent this diversity is affected by processing of IOM on the parent bodies. The fraction of aliphatic C compared to aromatic C decreases from CR2 through CI1, CM2 to Tagish Lake, while the content of O-bearing aliphatic functionalities increases (*Cody and Alexander,* 2005). However, *Gardinier at al.* (2000) reported higher aromaticity for the Orgueil (CI1) IOM compared to the Murchison (CM2) IOM.

These compositional and structural differences may also result in optical diversity of meteoritic IOM. The optical differences should be especially obvious between metamorphosed IOM from anhydrous meteorites and more primi-

tive IOM from hydrated meteorites. The IOM from metamorphosed chondrites is highly carbonized, i.e., highly absorbing through the VNIR spectral range without any IR absorption features, while IOM from type 1 and 2 meteorites should be more transparent in the VNIR and shows a number of IR absorption bands (e.g., *Gardinier et al.,* 2000). However, optical variations may exist even between such more primitive IOM among different hydrated meteorites classified as types 1 and 2. It is obvious that the scarce available optical data on meteoritic organic residues cannot fully represent the optical diversity inherent to meteoritic organics.

The IOM content may be as high as 40 wt.% in some IDPs, but their tiny sizes make it very difficult to extract organic matter in quantities sufficient for optical measurements. Infrared transmittance spectra of organic acid residues from several IDPs have been published by *Brownlee et al.* (2000) (3.2–3.7 μm) and *Flynn et al.* (2004) (5–14 μm). Raman spectroscopy revealed the polyaromatic character of IOM from IDPs (*Wopenka,* 1988; *Quirico et al*., 2005). Recent studies indicate that organic matter in both hydrated and anhydrous IDPs is very complex, resembling CI and CM IOM (*Flynn et al.,* 2003, 2004), while earlier studies suggested that most of the carbonaceous matter in anhydrous IDPs is represented by elemental amorphous carbon (*Keller et al.,* 1994). The complexity of organic matter in anhydrous IDPs is the direct evidence for the importance of indigenous complex organic matter for solar system objects formed beyond the "snow line," and not affected by aqueous alteration (*Flynn et al*., 2003), suggesting that indigenous complex organics may also be important constituents of some TNOs and Centaurs. Dust particles captured from a Jupiter-family comet, 81P/Wild 2, by the Stardust spacecraft are probably the most relevant to TNOs compared to all other extraterrestrial samples available to date. Organic components of the returned samples resemble organic matter from primitive meteorites and IDPs but are relatively poor in IOM and rich in labile soluble components (*Sandford et al.,* 2006). In addition, the Stardust organics seem to be depleted in aromatics and enriched in aliphatics (probably long-chain ones) as well as in O- and N-functionalities compared to known meteoritic and IDP organic matter (*Sandford et al.,* 2006; *Keller et al.,* 2006). Infrared transmittance spectra of some organic-rich comet grains and aerogel tracks in the 3.4-μm spectral region have been published by *Sandford et al.* (2006) and *Keller et al.* (2006).

More accessible terrestrial organics have also been considered as analog materials. Natural kerogens from terrestrial sedimentary rocks may be useful analogs. *Hayatsu et al*. (1983), *Ehrenfreund et al.* (1991), and *Murae* (1994) noted compositional, structural, and spectral similarities between meteoritic IOM and relatively evolved terrestrial kerogens of type III. However, some differences have also been reported (*Ehrenfreund et al.,* 1991; *Binet et al.,* 2002, 2004; *Quirico et al.,* 2003). Kerogens show significant diversity in terms of composition and chemical structure, even within a single type-I, II, or III, depending on maturation grade and/or variations in the organic precursors. For example, the composition, chemical structure and optical properties of a young type II kerogen are significantly different from those of an evolved (mature) type II kerogen. Again, optical constants (0.15–40 μm) are available only for a single sample of the type II kerogen (*Khare et al.,* 1990b). However, for these last experiments, the demineralization procedure has been performed before the removal of the bitumen fraction, so that the latter could have reacted with acids (see above). In addition, the derived organic residue has been heated to 550°–750°C prior to optical measurements, which could have produced further alteration of the residue. Similar concerns exist regarding the Murchison organic residue from the same work.

Infrared absorbance spectra (2.5–25 μm) of terrestrial kerogens have been published, e.g., by *Espitalié et al.* (1973), *Robin and Rouxhet* (1976), and *Rouxhet et al.* (1980), and, with astronomical applications, by *Ehrenfreund et al*. (1991) and *Papoular* (2001). Analysis of relative intensities of several absorption bands in the IR absorbance spectra allows one to assess a kerogen type and maturation degree (*Ganz and Kalkreuth,* 1987). *Papoular* (2001) draws parallels between spectral changes induced by kerogen maturation and evolution of organic-rich interstellar dust. No VNIR reflectance spectra of pure terrestrial kerogens (types I, II, III) have been published, to our knowledge. We expect the VNIR spectral slopes to decrease and NIR overtone and combination features to disappear with increasing maturation degree. It is also possible that relatively immature type III kerogens show redder VNIR slopes and less-pronounced NIR absorption features compared to immature type I and II kerogens (see discussion of coal optical properties below).

As noted above, a kerogen-like fraction can be derived from any kind of partly insoluble organic matter. For example, the USGS spectral database (*Clark et al.,* 1993) contains the VNIR (0.2–3 μm) spectrum of a chemically uncharacterized kerogen-like material derived by D. P. Cruikshank from a coal tar sample.

The properties of kerogens are affected by the procedures used for their isolation, while some other natural analogs described below exist in concentrated form. The so-called solid oil bitumens — asphaltites, kerites, and anthraxolites — constitute another group of natural complex hydrocarbon solids suggested as analog materials for extraterrestrial macromolecular polymers (*Moroz et al*., 1998, and references therein). The fraction of "kerogen" relative to the fraction of solvent-soluble bitumen, carbon aromaticity, and C/H ratio increase in this series from low-temperature asphaltites to thermally evolved high antraxolites. These changes are accompanied by a reduction of the spectral slope in the VNIR spectral range (Fig. 3). High kerites and low anthraxolites show compositional and structural similarities to organic matter from CM2 and CI1 chondrites, while high anthraxolites (shungites) resemble more carbonized organics of CV3 and CO3 chondrites. Reflectance spectra of solid oil bitumens between 0.5 and 17 μm have been published by *Moroz et al.* (1998), and transmittance spectra from 2.5 to 25 μm by *Moroz et al.* (1992). Optical constants (n and k) have been measured only for an asphaltite sample from 2.2 to 14 μm (unpublished data).

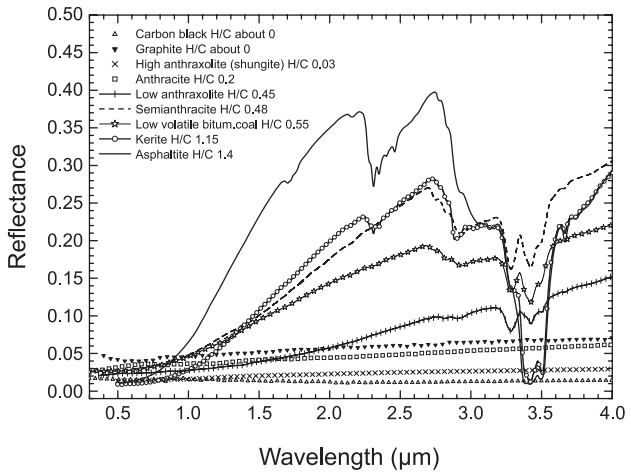

Fig. 3. Reflectance spectra of carbon black (90–125-μm powder); graphite (<45 μm), high rank coals (<100 μm) — low-volatile bituminous, semianthracite, and anthracite; solid oil bitumens (<25 μm) — asphaltite, kerite, low and high anthraxolites. The viewing geometry was biconical for solid bitumens (see *Moroz et al.,* 1998, for details); bidirectional (0.3–2.2 μm) and biconical (2.2–4 μm) for coals (spectra acquired at NASA RELAB facility); hemispherical for graphite (reproduced from the ASTER spectral library); hemispherical (0.3–2.7 μm) and biconical (2.1–4 μm) for carbon black (spectra acquired by R. Clark at the U.S. Geological Survey and J. Salisbury at Johns Hopkins University).

Natural coals of high ranks (low-volatility bituminous coals, semianthracites, anthracites) may also be useful analogs for extraterrestrial complex hydrocarbons (e.g., *Hayatsu et al.,* 1983; *Papoular et al.,* 1991, 1993; *Murae,* 1994; *Guillois et al.,* 1996). Low rank coals show additional NIR absorption features due to their high humidity and abundant mineral impurities (clays and carbonates), as shown in Fig. 4 for a lignite (brown coal) sample. Compared to solid oil bitumens with similar (H + O + N + S)/C ratios, coals are characterized by a higher degree of carbon aromaticity and are enriched in oxygen functionalities. As a result, NIR spectra of red bituminous coals and semianthracites lack absorptions at 2.3 μm and show much weaker absorptions at 3.4 μm compared to red bitumens, e.g., kerites (Fig. 3). Visible and near-IR spectral slopes of powdered carbonaceous materials with relatively high (H + O + N + S)/C ratios show significant dependence on particle size, as demonstrated in Fig. 4 for a lignite and a tholin sample, and in Fig. 2 from *Moroz et al.* (1998) for an asphaltite sample. This effect becomes less pronounced as the (H + O + N + S)/C ratios decrease. Reflectance spectra of some natural coals have been published by *Cloutis et al*. (1994) (0.3–2.6 μm) and *Cloutis* (2003) (0.3–26 μm). A number of authors published diffuse IR reflectance spectra of coal samples diluted in KBr or KCl. Many IR absorbance spectra of high rank natural coals have been published [e.g., *Painter et al.* (1985), 2.5–25 μm], some with astronomical applications [*Papoular et al.* (1991), 3–4 μm; *Guillois et al.* (1996), 3–15 μm; *Sourisseau et al*. (1992), 5–25 μm]. *Papoular et al.* (1991) published emissivity spectra of a semianthracite from 2 to 4.5 μm. Optical constants (n, k) of some coals have been obtained by *Van Krevelen* (1961) and *Papoular et al.* (1993) in the visible and by *Foster and Howarth* (1968) in the IR (1–10 μm).

Graphite — a very stable carbon allotrope composed of flat sheets of C atoms bonded into hexagonal structures — may form at the final stage of thermal evolution of natural organic solids such as coals, kerogens, solid oil bitumens, or meteoritic IOM. Visible and near-IR (0.3–2.6 μm) reflectance spectra of graphites (Fig. 3) have been published and discussed, e.g., by *Cloutis et al.* (1994). Fullerenes (large C molecules, e.g., C_{60}) are similar in structure to graphite but contain pentagonal or heptagonal rings. Fullerenes were detected in carbonaceous meteorites (*Becker et al.,* 1993, 1999; *Pizzarello et al.,* 2001) in low concentration of ~0.1 ppm. Fullerenes and buckyonions (multishell fullerenes) may be responsible for some UV and NIR bands in the ISM spectra (*Iglesias-Groth,* 2004, and references

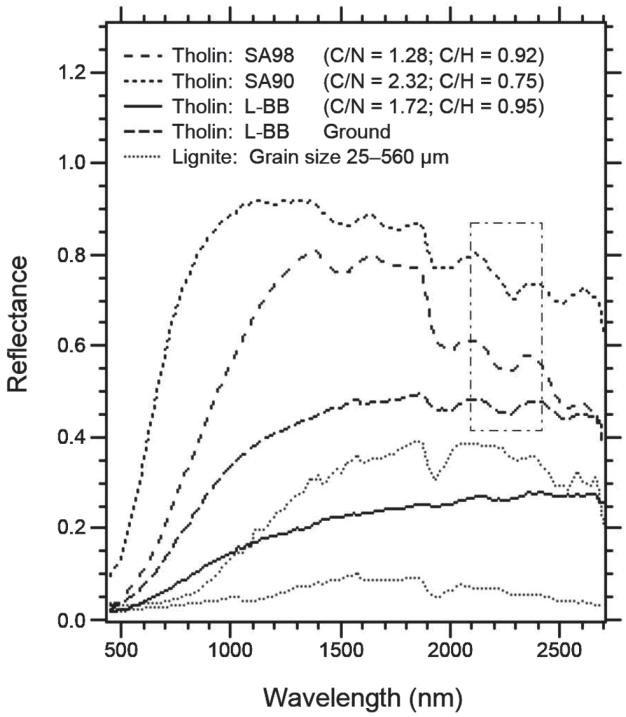

Fig. 4. Bidirectional reflectance spectra of Titan tholins and lignite (PSOC1532 Penn State Data Bank) coals (i = 0°, e = 30°). SA90 and SA98 tholins (two top curves) produced from the PAMPRE experiment (Service d'Aéronomie, Verrières-le-Buisson, France, courtesy of C. Szopa and G. Cernogora) have similar grain size distributions, but different chemical structures (*Szopa et al.,* 2006). The L-BB tholin is described in *Bernard et al.* (2006). This sample has also been ground in order to illustrate the effect of grain size. Note significant grain size effects and differences in the visible reflectance level and in the NIR vibrational bands. In particular, the –CN overtone near 2.2–2.3 μm (enclosed in the box) is useful for discriminating between the samples. Unlike tholins, lignites are black in the visible. Their NIR spectra show a band near 1.9 μm due to physically adsorbed and chemically bound water, and weaker bands between 2.1 and 2.6 μm due to combinations of metal–OH and OH bands in clays (see section 4.1) as well as combinations and overtones of C–H fundamentals.

therein). Optical constants of graphites and transmission spectra of fullerenes have been compiled in the Jena–St. Petersburg Database of Optical Constants (JPDOC) (*http://www.astro.uni-jena.de/Laboratory/Database/jpdoc*) (*Henning et al.,* 1999).

Thus, a review of the data available for various extraterrestrial and terrestrial carbonaceous materials shows a substantial lack of data on optical constants needed for modeling the spectra of TNOs and Centaurs.

4.2. Synthetic Carbonaceous Materials

The commonly used synthetic carbon materials as analogs of extraterrestrial carbonaceous materials are amorphous carbons, the so-called tholins, some disordered carbons (e.g., carbon blacks), and some irradiation products (described in section 4.3). These compounds indeed belong to the extensively wide family of amorphous and disordered carbon, which share numerous physical, electronic, and chemical properties. This section presents an overview of two classes of amorphous carbons of interest for analyzing TNOs spectral observations: pure and hydrogenated amorphous carbons and N_2:CH_4 (Titan and Triton) tholins. We particularly emphasize the physical and chemical control of their optical properties, and their potential use by astronomers.

4.2.1. Control of optical properties. Amorphous carbons and tholins can be considered as amorphous semiconductors. Their optical gap and electronic density of states, and therefore their optical properties in the visible and very-near-IR, are controlled by both the sp^2/sp^3 ratio and sp^2 structure. Note that sp^2 bonding is not restricted to aromatic species as in polyaromatic organics (coals, kerogens, etc.), and may include olefinic carbons in short chains, imides, etc.

The absorption in the visible range consists in a broad continuum, with the imaginary part of the refractive index related to the joint density of states (JDOS), which considers all types of π-π^* electronic transitions (*Knief and von Niessen,* 1999). Therefore, the parameters that control the spectral shape of this continuum are very complex and cannot be restricted to the Tauc or E_{04} gap, nor to the abundance and/or size of aromatic units. This explains why large spectral variations are reported from one compound to another (*Logothedis et al.,* 1995), thus frustrating attempts to derive physical information from the shape and/or slope of reflectance data in the visible.

In contrast, the spectral region from the near-IR to the far-IR is dominated by vibrational bands with no broad continuum. These are the bands that are the most interesting for identifying a specific compound, or to describe the chemical structure. The major limitation of using them comes from the spectral complexity due to the superimposition of numerous bands in complex macromolecular materials.

4.2.2. Amorphous carbons and hydrogenated carbons. Pure and hydrogenated amorphous carbons have been widely used as darkening agents in reflectance modeling of low-albedo solar system objects, and may be considered as analogs of irradiation products. Pure amorphous carbons constitute a wide range of carbon allotropes, which are classified according to their sp^2/sp^3 and their sp^2 structure, defined as the nature and extent of clustering and ordering of the sp^2 carbon bonds (*Ferrari and Robertson,* 2000).

Amorphous carbons are generally subdivided in two forms: (1) amorphous carbons (a-C), which are described as graphite-like sp^2 rich compounds; and (2) tetrahedral amorphous carbons (ta-C), described as sp^3-rich diamond-like carbons (DLC). A wide variety of compounds can be obtained in the laboratory, by using different deposition setups and/or experimental conditions, or by performing heating experiments on various precursor materials (*Beny-Bassez and Rouzaud,* 1985; *Logothetidis et al.,* 1995). Hydrogenated amorphous carbons contain up to 60% H, above which no solid can be formed, and are classified according to the same parameters as amorphous carbons, supplemented by the H/C ratio (*Ferrari and Robertson,* 2000). Introducing hydrogen within the carbon structure leads to the formation of sp^3 CH bonds. The general framework for interpreting their electronic structure and optical properties is similar to that applied to pure amorphous carbons. Note that tholins (see below) formed from CH_4 gas are indeed largely hydrogenated amorphous carbons (e.g., *Khare et al.,* 1987; *Mutsukura and Akita,* 1999), although aromatic and aliphatic structures, both with varying degrees of N substitution, are found in them (e.g., *Imanaka et al.,* 2004; *Bernard et al.,* 2006).

Only a few vibrational bands are present in the IR spectra. In the mid-IR, a broad and intense feature is reported at ~1250 cm^{-1} (~8 μm), associated with a weaker one at ~700 cm^{-1} (~14.3 μm) (*Rodil et al.,* 2001). The intensities of these features are correlated with the sp^2 content, therefore their IR activity has been interpreted by the presence of dynamic charges, allowed by the lack of local symmetry and the extent of conjugated π bonds (*Rodil et al.,* 2001, 2003). No overtones of these features have yet been reported in the near-IR, although they might be expected. No other features are detected in the far-IR for wavenumbers shorter than 400 cm^{-1} (>25 μm). Hydrogenated amorphous carbons furthermore present typical IR features of the CH_2 and CH_3 functional groups, as the well-known features around 2900 cm^{-1} (3.4 μm), plus the aromatic C–H stretching mode at 3040 cm^{-1} (3.29 μm) (e.g., *Schnaiter et al.,* 1999; *Pendleton and Allamandola,* 2002).

Many studies have been focused on the determination of optical properties of amorphous carbons (e.g., *Rouleau and Martin,* 1991; *Compagnini,* 1994; *Roush,* 1995), but few of them provide tabulated values of optical constants (*Arakawa et al.,* 1985; *Preibisch et al.,* 1993; *Zubko et al.,* 1996; *Jäger et al.,* 1998a). A major concern of astronomers is the selection of the most relevant sets of data. Indeed, large variations are reported among optical data from different studies and/or different kinds of carbons. For instance, the imaginary part (k) of the refractive index varies by more than two orders of magnitude within the data from *Arakawa et al.* (1985), *Preibisch et al.* (1993), and *Jäger et al.* (1998a).

Such variations reflect the wide diversity of amorphous carbons, and raise the problem of the selection of datasets.

The lack of systematic studies of the connection between optical properties and structural state of amorphous carbons also complicates the problem. Consequently, it is more prudent to select end members of various sets of data, in order to account for both absorption strength and spectral variations in the visible range. As noted above, no reliable information on surface composition can be derived from the slope of the visible reflectance curve, although the reddest surfaces cannot be explained by plausible minerals and thus require the presence of organic materials (*Cruikshank et al.,* 2001, 2005a,b).

4.2.3. N_2:CH_4 tholins. Tholins are complex organic compounds formed from initial gaseous mixtures exposed to electrical discharge or energetic photons. Various experiment configurations have been dedicated to studies of planetary relevance, including synthesis in cold plasma generated by a radio-frequency source (e.g., *Imanaka et al.,* 2004; *Szopa et al.,* 2006), spark discharge (*Khare et al.,* 1984), direct current discharge (e.g., *Coll et al.,* 1999), or purely ultraviolet light (*Ferris et al.,* 2005; *Tran et al.,* 2003). Various initial gaseous mixtures have been used, including numerous combinations of N_2, NH_3, CH_4, and H_2O. Ice tholins are compounds formed from irradiation of ice samples, and are described below along with other irradiation products. Note that tholins formed from gaseous mixtures are not strictly irradiation products, but are nevertheless used as analogs of irradiated ices present at the surface of TNOs or icy satellites. N_2:CH_4 has been by far the most extensively investigated mixture, because of its interest for simulating the atmospheric aerosols of Titan. Somewhat different are Triton tholins, which are formed from N_2:CH_4 mixtures with low CH_4 concentration (more relevant to Triton's atmosphere), but they are considered here in context with Titan tholins (*McDonald et al.,* 1994). We restrict the discussion in this section to N_2:CH_4 tholins due to the fact that they received much attention and that optical data are available.

N_2:CH_4 tholins are simply "polymer-like" amorphous hydrogenated carbon nitrides (e.g., *Mutsukura and Akita,* 1999; *Bernard et al.,* 2006). The term "tholin" was originally coined specifically to describe the materials synthesized in the context of organic materials in interstellar dust and planetary environments (*Sagan and Khare,* 1979), and is explicitly defined as organic solids produced by the irradiation of mixtures of cosmically abundant reducing gases (*Sagan et al.,* 1984). Compounds of this general type are rather common in materials science, and have been widely investigated using numerous techniques. Generally speaking, the classification scheme used for a-C and a-C:H compounds extends to any form of carbon nitrides, using the C/N ratio and N speciation as key factors controlling the chemical structure and sp^2 clustering. Nitrogen may present various sp^1, sp^2, and sp^3 bonding configurations with carbon, and also bonds with hydrogen as the amine functions $–NH_2$ and –NH–. As for other amorphous carbons, the system deposition and experimental parameters play a key role in the structure and composition of the materials. Four general classes of carbon nitrides have been defined for a current usage in materials science (*Rodil et al.,* 2001; *Ferrari et al.,* 2003). N_2:CH_4 tholins do not belong to any of these classes, but as noted above, can be described as a class of "polymer-like" hydrogenated carbon nitrides.

Numerous optical data are available for N_2:CH_4 tholins and in-depth systematic studies have revealed general trends in the control of samples' elemental composition, chemical structure, and optical properties with various experimental parameters: gas composition, pressure, discharge setup, injected power, and temperature (*McDonald et al.,* 1994; *McKay,* 1996; *Imanaka et al.,* 2004; *Bernard et al.,* 2006). The chemical structure of these compounds is not fully elucidated, however. Unlike other amorphous carbon nitrides, N_2:CH_4 tholins contain numerous functional chemical groups, as evidenced by their feature-rich IR spectra (*Imanaka et al.,* 2004; *Bernard et al.,* 2006; *Quirico et al.,* 2006) (see also Fig. 4). Therefore, optical properties in the IR range are controlled by the chemical composition, whereas the absorption in the visible and very near-IR is controlled by the sp^2 structure and the sp^2/sp^3 ratio. These latter are indeed correlated with the C/N ratio, as nitrogen favors sp^2 clustering. Finally, the so-called "HCN polymer" can be discussed with N_2:CH_4 tholins. This compound has been suggested as a widespread nitrogen-rich organic material in the solar system (e.g., *Minard et al.,* 1998). It is indeed an amorphous hydrogenated carbon nitride with a chemical structure similar to, but distinct from, that of N_2:CH_4 tholins (*Quirico et al.,* 2006).

We note that *Khare et al.* (2002) studied the time-dependent composition and structure of a N_2:CH_4 tholin, as well as chemical effects of exposure to oxygen and to laboratory air. Exposure to oxygen and moist air had no effect on the basic composition and structure of tholin, except to produce a weak absorption band attributed to CO_2 (2299–2398 cm^{-1}; 4.17–4.35 μm), and to remove (by oxidation) an aromatic C–H band around 3030 cm^{-1} (3.30 μm). These changes produced negligible differences in the pre- and post-exposure IR spectra, and changes in the optical constants would also therefore be negligible.

Among the sets of optical constants of N_2:CH_4 tholins available in the literature are those of *Khare et al.* (1984), *Ramirez et al.* (2002), *Tran et al.* (2003), and *Imanaka et al.* (2004). Within a series of tholins derived from similar experimental conditions by only varying the cell pressure, *Imanaka et al.* (2004) have shown that systematic variations of the optical constants arise. Indeed, tholins formed in different experimental configurations exhibit variations in their chemical structures, resulting in significant variations in their optical constants (e.g., *Ramirez et al.,* 2002; *Tran et al.,* 2003; *Imanaka et al.,* 2004). Therefore, the range of variations of optical properties of tholins should not be considered as a linear continuum, but rather as sets of data incoming from similar, but distinct, samples and experimental setups. For these reasons, as pointed out above for amorphous carbons, it appears relevant to select end members

of available sets for modeling. This is of particular importance for fitting observational data in the visible spectral range. Additional focused efforts are needed to obtain measurements of optical constants along with in-depth structural and chemical characterization of samples of carbon nitrides in order to make significant advances in our knowledge of the chemical and structural control of the optical properties.

Reflectance spectra of tholins and HCN polymer have been published by *Cruikshank et al.* (1991, 1995), *Roush and Dalton* (1994), and *Bernard et al.* (2006) in which a wide variety of overtone and combination bands is observed in the near-IR (see, e.g., Fig. 4). These features, used along with the reflectance in the visible region, are valuable fingerprints of the chemical structure of N-rich organics. The 2.2-μm feature, which is the first overtone of the stretching modes of the –CN and –NC functional groups, may be particularly useful as a clue to the chemical structure. Indeed, the ~4.6-μm fundamental band has been proved as an interesting tracer of the C/N ratio within a series of tholins obtained from the same experimental configuration, and also helps to discriminate tholins from the so-called "HCN polymer" (*Imanaka et al.,* 2004; *Quirico et al.,* 2006). The visible reflectance, which consists mostly of a reddish monotonic curve, may also be useful. There is a rough correlation with the highest reflectance value and the spectral depth and position of the bands in the near-IR. This is evidence for a correlation between the optical gap controlling the visible absorption and the chemical structure and C/N ratio. Finally, the shape and position of the CN/NC 2.2-μm overtone, the absence or presence of CH_2/CH_3 and/or NH/NH_2 chemical function bands, together with the reflectance in the visible, should be considered as valuable fingerprints of "polymer-like," hydrogenated carbon nitrides.

4.3. Irradiation Products

Irradiating C-bearing ices, refractory hydrocarbon solids, and ice-refractory hydrocarbon mixtures with energetic particles or photons leads to their chemical, structural, and optical transformation to refractory carbonaceous materials. CH_4 ice may transform to a-C:H when irradiated by Lyman-α photons (*Dartois et al.,* 2005). Numerous studies have demonstrated the formation of amorphous or disordered carbons from ion irradiation experiments (see chapter by Hudson et al.). Most of these studies, reviewed by Hudson et al., demonstrate that amorphous carbons can be considered as valuable analogs of carbon-bearing irradiation products, although few optical constants are available. The so-called ice tholins are solids produced from icy samples exposed to plasma irradiation (*McDonald et al.,* 1991, 1996; *Khare et al.,* 1993). Different mixtures lead to solids with different chemical composition as evidenced by their IR spectra. These solids exhibit numerous oxygenated chemical functional groups, and they can be used as analogs of irradiation products of hydrocarbon ices containing water, or oxygen-bearing molecules like methanol in planetary conditions. Optical constants (measured at room temperature) are available for one ice tholin obtained from a C_2H_6/H_2O mixture irradiated at 77 K (*Khare et al.,* 1993).

5. MINERALS

At present, information on plausible mineral components of TNOs and Centaurs is based mostly on our knowledge of the composition of cometary dust and "cometary" (anhydrous "chondritic porous") IDPs. These data suggest Mg-rich anhydrous crystalline mafic silicates — forsterite and enstatite — as the most plausible major silicate components, and iron sulfides (e.g., troilite FeS, pyrrhotite $Fe_{1-x}S$) as the most plausible major non-silicate minerals (e.g., review by *Wooden et al.,* 2005, and references therein; *Zolensky et al.,* 2006; chapter by Gounelle et al.). Forsterite is the Mg-member of the olivine series (forsterite Mg_2SiO_4–fayalite Fe_2SiO_4), while enstatite is the Mg-member of low-Ca pyroxene series (enstatite $MgSiO_3$–ferrosilite $FeSiO_3$). Data on Fe^{2+}-bearing olivines and pyroxenes are also reviewed below, since such minerals, which are common components of many meteorites and asteroids, may also be present on TNOs and Centaurs; Fe^{2+}-bearing olivine significantly improved spectral models of Pholus around 1 μm (*Cruikshank et al.,* 1998), and *Lisse et al.* (2006) reported detection of Fe-rich pyroxene (ferrosilite) in Spitzer Space Telescope (SST) spectra of Comet 9P/Tempel 1 acquired during the Deep Impact encounter. In addition, a wide range of olivine and low-Ca pyroxene compositions has been detected in anhydrous IDPs and samples returned by the Stardust mission, although Mg-rich crystalline forsterites and enstatites were the most abundant silicates (*Zolensky et al.,* 2006). Anhydrous crystalline mafic silicates clearly dominate the silicate fraction in solar system materials and protoplanetary disks, while amorphous Fe-bearing silicates are abundant in the ISM, and some fraction of cometary silicates seems to be amorphous according to IR observations (*Wooden et al.,* 2005). Along with crystalline silicates, "cometary" IDPs contain glass with embedded metal and sulfides (GEMS) — spherules of uncertain origin, composed of amorphous Mg, Fe,Al,Si-silicate with embedded iron sulfides and Fe-metal grains (*Dai and Bradley,* 2005). Amorphous GEM-like particles with IR spectra resembling those of the ISM amorphous silicates (*Keller et al.,* 2006) are also present in Stardust mission samples, although it is not yet clear whether any fraction of the detected amorphous silicates existed before collection (*Brownlee et al.,* 2006; *Zolensky et al.,* 2006). In any case, data on amorphous anhydrous minerals are also discussed below.

No unambigous detections of hydrated minerals (e.g., serpentines, smectites) in comets have been reported (*Wooden et al.,* 2005). *Lisse et al*. (2006) reported emission features due to carbonates and hydrated silicates in the SST spectra of Comet 9P/Tempel 1, while none of these minerals have been detected in the samples returned by Stardust (*Brownlee et al.,* 2006; *Zolensky et al.,* 2006). However, such phases are abundant in primitive meteorites and some IDPs (see

chapter by Gounelle et al.), and weak features possibly related to phyllosilicates have been reported for several TNOs and Centaurs (see chapter by Barucci et al.), although confirmation is needed. Therefore, we briefly mention some data on hydrated minerals as well.

Difficulties in detecting silicate features in the VNIR spectra of TNOs and Centaurs may be either due to the opacity of associated carbonaceous species and sulfides in this spectral region, or to the lack of Fe^{2+} in the silicates (see below). Recent SST detection of silicates on 8405 Asbolus (see chapter by Barucci et al.) and several Trojans (*Emery et al.,* 2006) shows that the thermal-IR region (TIR) ($\lambda >$ 10 μm) is potentially useful for silicate detection on TNOs and Centaurs, therefore we include TIR data on relevant minerals in this review.

5.1. Crystalline Olivines and Pyroxenes

Mid- and far-IR data on crystalline olivines and pyroxenes of various Fe/(Fe + Mg) contents have been compiled in JPDOC (*Henning et al.,* 1999). Mid-IR optical constants (at room temperature) have been published for crystalline olivines [e.g., *Mukai and Koike* (1990), 7–200 μm; *Fabian et al.* (2001), 8–130 μm], and for crystalline low-Ca pyroxenes [e.g., *Roush et al.* (1991), 5–25 μm; *Jäger et al.* (1998b), 5–100 μm]. *Henning and Mutschke* (1997) published optical constants of a Fe-bearing pyroxene (bronzite) sample between 6.7 and 500 μm as a function of temperature. Olivines show strong diagnostic absorption bands between 9 and 12 μm (Si-O stretches) as well as a number of other bands at longer wavelengths, which shift to shorter wavelengths with decreasing Fe/(Fe + Mg) content (e.g., *Koike et al.,* 2003) and temperature (*Koike et al.,* 2006). Pyroxene Si-O vibrations occur at somewhat shorter wavelengths and pyroxenes show more bands than olivines, especially Mg-rich pyroxenes, most of which shift to shorter wavelengths with decreasing Fe/(Fe + Mg) content, while the 10.5- and 11.5-μm bands shift to longer wavelengths (*Chihara et al.,* 2002).

Infrared reflectance spectra (2–25 μm) of crystalline olivines and pyroxenes of various compositions and several grain size ranges can be found in the ASTER spectral library (*http://speclib.jpl.nasa.gov*). The contrast of diagnostic IR features in reflectance and emittance spectra is strongly affected by grain size (*Lyon,* 1964).

Few laboratory mid-IR emissivity spectra exist for crystalline olivines and pyroxenes: spectra of coarse (710–1000 μm) olivine (forsterite and fayalite) and pyroxene separates from the Arizona State University (ASU) spectral library (*Christensen et al.,* 2000); spectra of forsterite fines (from <5 to 20–25 μm) from *Mustard and Hays* (1997); and spectra of forsterite, diopside, and Fe-bearing enstatite separates (from <25 to 125–250 μm) from the BED library (*Maturilli et al.,* 2007). Note that these measurements were made at ambient pressure, while emissivity spectra may be significantly different at low pressures (*Logan and Hunt,* 1970). Analysis of Spitzer observations of Trojans shows a need for laboratory IR emissivity data on hyperfine silicates (including crystalline and amorphous olivines and pyroxenes) and Fe-free silicates (*Emery et al.,* 2006).

Most observations of TNOs and Centaurs are made in the VNIR spectral range. Near-IR spectra of crystalline olivines are characterized by three overlapping absorptions around 1 μm due to crystal field transitions in the Fe^{2+} ion (*Burns,* 1970). Major Fe^{2+} crystal field absorptions occur in the spectra of pyroxenes at 0.9–1.15 μm (band I) and 1.8–2.3 μm (band II) (*Burns,* 1970; *Adams,* 1974). Wavelength positions and contrasts of Fe^{2+} bands increase with increasing Fe content (olivines and pyroxenes) and Ca content (pyroxenes), while the band widths and relative contrasts in VNIR reflectance spectra are affected not only by composition but also particle size (*Burns,* 1970; *Adams,* 1974; *King and Ridley,* 1987; *Cloutis and Gaffey,* 1991; *Sunshine and Pieters,* 1998). Room-temperature VNIR reflectance spectra (0.3–2.5 μm) of various crystalline olivines and pyroxenes are available in the USGS (*Clark et al.,* 1993) and RELAB (*Pieters and Hiroi,* 2004) spectral libraries and a number of publications. Very few data exist on VNIR optical constants of olivines and pyroxenes. *Lucey* (1998) derived k values from published olivine and pyroxene reflectance spectra. These data extend only to 2.3 or 2.5 μm. Terrestrial mafic minerals often contain some weathering products, fluid inclusions and adsorbed water, which affect the spectra beyond 2.2–2.3 μm and especially around 3 μm. However, modeling of observed TNO and Centaur spectra often requires optical constants covering wider spectral ranges (e.g., *Cruikshank et al.,* 1998). Optical constants from *Huffman and Stapp* (1973) (n: 0.08–8 μm), *Huffman* (1975) (k: 0.03–300 μm), and *Pollack et al.* (1994) (0.1–10^5 μm) are available for crystalline olivines, and only from *Pollack et al.* (1994) (0.1–10^6 μm) for crystalline orthopyroxene. No VNIR optical constants have been published for "featureless" pure Fe-free crystalline forsterites and enstatites, whose VNIR optical properties are dramatically different from those of crystalline Fe-poor forsterites and enstatites (e.g., *Adams,* 1975; *Cloutis et al.,* 1990). No VNIR optical constants have been measured at low T relevant to TNOs and Centaurs, while VNIR reflectance spectra of Fe-bearing crystalline olivines and pyroxenes are known to be affected by temperature (*Singer and Roush,* 1985; *Moroz et al.,* 2000; *Hinrichs and Lucey,* 2002).

5.2. Amorphous Olivines and Pyroxenes

Few data exist on amorphous pyroxenes and olivines, since natural samples are unavailable, and laboratory production is difficult. Amorphized olivines and pyroxenes for optical studies are usually produced by evaporation (*Koike and Tsuchiyama,* 1992), laser ablation (*Scott and Duley,* 1996; *Fabian et al.,* 2000; *Brucato et al.,* 1999, 2002), reactive sputtering (*Day,* 1979, 1981), or irradiation with low-energy ions (*Brucato et al.,* 2004). These publications show IR spectra of amorphous olivines and/or pyroxenes in trans-

mittance or absorbance. Amorphous olivines and pyroxenes show a broad smooth absorption band centered near 10 μm and a weaker broader band around 20 μm. Optical constants of amorphous olivines and pyroxenes have been published by *Day* (1979) (forsterite and enstatite, 7–33 μm), *Day* (1981) (fayalite and ferrosilite, 7–300 μm), *Scott and Duley* (1996) (forsterite and enstatite, probably Fe-bearing, 0.12–17.5 μm), *Henning and Mutschke* (1997) (pyroxene glass, 6.7–500 μm). *Dorschner et al.* (1995) published optical constants of Mg-Fe-silicate glasses of olivine and pyroxene composition between 0.2 and 500 μm. Visible and near-IR optical properties of mafic glasses are strongly affected by cooling rate and oxygen fugacity of the ambient atmosphere. *Dorschner et al.* (1995) produced their glasses in air, so that a large fraction of the Fe^{2+} was oxidized to Fe^{3+}. Oxidation does not significantly affect the mid- and far-IR spectra (*Ossenkopf et al.,* 1992), but Fe^{3+} produces very strong absorption from the UV through the VNIR range, causing darkening and a steep red slope in the VNIR range. Basically, VNIR optical data of acceptable quality on pure amorphous olivines, which could be used in TNO and Centaur spectral models, are currently unavailable. For amorphous pyroxenes in the VNIR spectral range, only Fe-free pyroxene glass from *Dorschner et al.* (1995) is a reasonable simulation of a pure amorphous silicate.

5.3. Hydrated Minerals

The presence of hydrated minerals at the surface of TNOs has been suggested (see chapter by Barucci et al.). Although on Earth there is a vast range of hydrated minerals, not all terrestrial hydrated minerals are relevant to TNOs, which are thought to be largely primitive. Consequently, the most logical minerals to investigate through modeling are those found in pristine chondritic meteorites, IDPs, or the comet grains collected by the Stardust mission. However, no hydrated minerals have yet been detected in the comet samples returned by Stardust, and their absence cannot be explained by dehydration during capture (*Zolensky et al.,* 2006).

A number of hydrated minerals are plausible components of TNOs, such as phyllosilicates, salts, and hydrated oxides. The NIR spectral properties of hydrated minerals are dominated by features due to H_2O (~1.4, ~1.9, ~3 μm) and structural OH. The wavelengths of OH (~1.4, ~2.7 μm) and metal-OH (2.2–2.4 μm) bands in phyllosilicates are controlled by their cationic compositions (e.g., *Bishop et al.,* 2002a,b), resulting in a wide range of possibilities. Unlike ices, the identification of a specific mineral is often uncertain and cannot normally be accomplished with only one series of reference spectra. Reference spectra covering a wide range of compositions within a specific mineral type are essential.

The complicating effects are illustrated by a specific example: Fe^{3+}-bearing phyllosilicates may show absorption features near 0.43 μm and 0.6–0.8 μm, but these features are not diagnostic of hydrated silicates since bands at similar wavelengths are found in reflectance spectra of numerous *anhydrous* minerals. Such features may be assigned to hydrated minerals only if corresponding NIR absorption bands noted above are also present.

Visible and near-IR optical constants of relevant hydrated minerals are largely unavailable. *Bishop et al.* (2002a,b) have investigated the effect of cationic compositions on IR spectra of phyllosilicates, while reflectance spectra of hydrated oxides and sulfates have been published by *Bishop et al.* (1993) and *Cloutis et al*. (2006), respectively, and references for carbonates can be found in *Calvin et al.* (1994).

5.4. Irradiated Silicates

The possible contribution of irradiated silicates to VNIR optical properties of TNOs and Centaurs is an open question. Irradiation with low-energy solar wind plasma may darken and redden Fe-bearing silicates. Sputtering of Fe from silicate targets and its redeposition, causing darkening and reddening in experiments with high ion fluences (reviewed by *Hapke,* 2001), may be negligible for TNOs and Centaurs. Ion irradiation experiments on silicates, performed by the Catania group at low ion fluences (see chapter by Hudson et al.), where darkening and reddening are caused by radiation damage induced by elastic collisions in a thin (<1 μm) surface layer of silicates, seem to be more relevant. It is unclear whether optical effects of irradiation are negligible in the case of Fe-free silicates, since the possible role of Fe in the latter experiments remains to be clarified. Available data show that even very Fe-poor silicate samples darken and redden under irradiation, but no experiments have been performed on pure Fe-free silicate targets. Another question concerns the relative rates of irradiation-induced silicate darkening and reddening compared to the rates of competing regolith gardening on TNOs and Centaurs. Before we know the answers to these questions, we may consider irradiated silicates as possible end members in some TNOs/Centaur spectral models and simulate space-weathering effects by incorporation of fine Fe inclusions into silicate grains.

5.5. Iron Sulfides

Iron sulfides, sometimes enriched in Ni, such as pyrrhotite and troilite, are common opaque components of meteorites, IDPs, and cometary dust (*Jessberger et al.,* 1988; *Zolensky and Thomas,* 1995; *Schulze et al.,* 1997; *Zolensky et al.,* 2006). Infrared spectra of iron sulfides show a characteristic feature at ~23–24 μm (*Keller et al.,* 2002) and several weaker features at longer wavelengths (*Hony et al.,* 2002; *Kimura et al.,* 2005). Similar bands have been detected in IR spectra of planetary nebulae and C-rich stars (*Forrest et al.,* 1981) and assigned to sulfides (*Keller et al.,* 2002; *Hony et al.,* 2002). *Henning and Mutschke* (1997) published n and k of FeS from 10 to 500 μm. At wavelengths <23 μm iron sulfides are featureless, except for OH-bearing tochilinites, which are the most abundant sulfide phases in CM2 chondrites and show features near 2.7–2.8 μm due to O-H stretches (*Moroz et al.,* 2006). Visible

and near-IR reflectance spectra of relevant sulfide powders have been published by *Britt et al.* (1992) (troilite), *Cloutis and Gaffey* (1993) (troilite, pyrrhotite), and *Moroz et al.* (2006) (tochilinite). Like other opaque semimetals, sulfide powders become darker with decreasing grain size. Troilite and pyrrhotite powders containing coarse grains show reddish slopes in reflectance spectra and may redden mixtures with other phases if present in high quantities. Fine (submicrometer) Fe sulfide grains do not redden but effectively darken a mixture with bright phases and suppress their VNIR absorption features. For example, in CM2 chondrites sulfide fines appear to be the most important darkening phases. *Egan and Hilgeman* (1977) published optical constants of troilite and pyrrhotite between 0.3 and 1.1 μm. *Pollack et al.* (1994) reported n and k of troilite from 0.1–10^5 μm, but the values between 1.1 and 3 μm and below 0.3 μm were estimated by extrapolation. New values of n and k of troilite between 0.1 and 10^5 μm, measured by the Jena group, can be found at *www.mpia-hd.mpg.de/homes/henning/Dust_opacities/Opacities/RI/troilitek.lnk.*

5.6. Iron-Nickel Metal

Metallic Fe or Fe,Ni alloys are usually only minor components of carbonaceous chondrites, IDPs, and comets, but tiny Fe metal particles may be products of space weathering of Fe-bearing silicates and therefore the data on iron metals are briefly summarized here. Similar to other metals, metallic iron is opaque and shows continuous featureless absorption from UV to FIR. Optical constants for various spectral ranges are summarized in the JPDOC database (*Henning et al.,* 1999). Visible and near-IR reflectance spectra of Fe,Ni from meteorites show an increase in reflectance as a function of wavelength (e.g., *Gaffey,* 1976; *Cloutis and Gaffey,* 1993). Fine metallic iron particles cause darkening and reddening of "space-weathered" Fe-bearing silicates and suppress absorption bands in their VNIR spectra (*Hapke,* 2001, and references therein).

6. CONCLUSION

We have reviewed the available laboratory data on detected or plausible TNOs and Centaurs surface materials. For each class of material (ices, refractory carbonaceous compounds, and minerals) we have indicated the laboratory data that are still missing. As we have seen, in many cases the materials of interest have been studied in some details only in the thermal-IR, while the near-IR and visible ranges are the most important ranges for TNOs and Centaurs. Furthermore, concerning the optical constants, which are required for a proper interpretation of the spectra, only very few are available for materials and conditions relevant to TNOs and Centaurs. In addition, very few studies of ice mixtures, and almost no study of mixtures of different classes of materials, have been made in the near-IR.

Concerning carbonaceous compounds, it is clear that the spectroscopic studies carried out so far do not cover the full range of possibilities. Other compounds should be studied in the VNIR, e.g., other carbon nitrides as well as other photolysis or radiolysis organic products (see also the chapter by Hudson et al.).

As we have noted, spectral slopes do not provide strong constraints on the surface composition because widely different classes of compounds can provide similar slopes (and shapes). However, investigators have been unable to find components other than complex refractory carbonaceous species to account for the very red colors of some TNOs. In particular, none of the plausible silicates that have been considered are red enough. Some classes of carbonaceous compounds with detectable features in their near-IR spectra, very often in the 2–2.5-μm region, have been noted. This is the case, for instance, of solid bitumens with relatively high H/C ratios, coals of not too high ranks, possibly relatively immature kerogens, and hydrogenated amorphous carbons with high H contents. In order to identify (or reject) these materials on TNOs, we therefore need spectra of higher signal precision (S/N), particularly in the spectral region 2–2.5 μm, than presently exist.

Another concern is the availability of the numerical files of the laboratory spectra and optical constants that have been obtained. Although a number of databases can be found on various websites (and these have been mentioned in the text), the existing databases are clearly insufficient. This is especially true for ices and organics. A major effort toward this aim, a website of spectroscopic data (transmission and reflectance spectra, optical constants, lists of absorption bands and attributions, etc.) of solid materials of planetary interest, including ices and organics, is currently under development at the Laboratoire de Planétologie de Grenoble (LPG) in France, and should begin providing data in 2008. Furthermore, recently acquired spectra of a number of hydrocarbons and other organic compounds will soon become available in digital form through the U.S. Geological Survey Spectroscopy Laboratory (R. N. Clark, personal communication). We encourage other people to do the same.

All these laboratory studies require important investments in laboratory equipment and the time of dedicated researchers. While new laboratory data are slow to materialize, thanks to new instrumentation, improved and more numerous data are becoming available for TNOs and Centaurs, showing their great diversity and the "richness" of this population. Furthermore, with the New Horizons mission, spatially resolved IR spectra of Pluto should become available in 2015. The spacecraft is expected to continue on to one or two TNOs, offering the possibility of spatially resolved spectra of these objects. It is therefore essential to carry out in parallel an ambitious program of laboratory spectroscopy.

REFERENCES

Adams J. B. (1974) Visible and near-infrared diffuse reflectance spectra of pyroxenes as applied to remote sensing of solid objects in the solar system. *J. Geophys. Res., 79,* 4829–4836.

Adams J. B. (1975) Interpretation of visible and near-infrared

diffuse reflectance spectra of pyroxenes and other rock-forming minerals. In *Infrared and Raman Spectroscopy of Lunar and Terrestrial Minerals* (C. Karr, ed.), pp. 91–116. Academic, New York.

Alexander C. M. O'D., Russell S. S., Arden J. W., Ash R. D., Grady M. M., and Pillinger C. T. (1998) The origin of chondritic macromolecular organic matter: A carbon and nitrogen isotope study. *Meteoritics & Planet. Sci., 33,* 603–622.

Arakawa E. T., Dolfini S. M., Ashley J. C., and Williams M. W. (1985) Arc-evaporated carbon films: Optical properties and electron properties and electron mean free paths. *Phys. Rev. B, 31,* 8097–8101.

Becker L., McDonald G. D., and Bada J. L. (1993) Carbon onions in meteorites. *Nature, 361,* 595.

Becker L., Bunch T. E., and Allamandola L. J. (1999) Higher fullerenes in the Allende meteorite. *Nature, 400,* 227–228.

Beny-Bassez C. and Rouzaud J-N. (1985) Characterization of carbonaceous materials by correlated electron and optical microscopy and Raman spectroscopy. *Scanning Electron Microscopy, 1,* 119–132.

Bernard J-M., Quirico E., Brissaud O., Montagnac G., Reynard B., McMillan P., Coll P., Nguyen M-J., Raulin F., and Schmitt B. (2006) Reflectance spectra and chemical structure of Titan's tholins. Application to the analysis of Cassini-Huygens observations. *Icarus, 185,* 301–307.

Bernstein M. P. and Sandford S. A. (1999) Variations in the strength of the infrared forbidden 2328.2 cm^{-1} fundamental of solid N_2 in binary mixtures. *Spectrochim. Acta, Part A, 55,* 2455–2466.

Bernstein M. P., Cruikshank D. P., and Sandford S. A. (2005) Near-infrared laboratory spectra of solid H_2O/CO_2 and CH_3OH/CO_2 ice mixtures. *Icarus, 179,* 527–534.

Bernstein M. P., Cruikshank D. P., and Sandford S. A. (2006) Near-infrared spectra of laboratory H_2O-CH_4 ice mixtures. *Icarus, 181,* 302–308.

Bertie J. E. and Devlin J. P. (1984) The infrared spectra and phase transitions of pure and isotopically impure $2ND_3.H_2O$, $2NH_3.D_2O$, $2NH_3.H_2O$, and $2ND_3.D_2O$ between 100 and 15 K. *J. Chem. Phys., 81,* 1559–1572.

Bertie J. E. and Shehata M. R. (1984) Ammonia dihydrate: Preparation, X-ray powder diffraction pattern and infrared spectrum of $NH_3.2H_2O$ at 100 K. *J. Chem. Phys., 81,* 27–30.

Bertie J. E. and Shehata M. R. (1985) The infrared spectra of $NH_3.H_2O$ and $ND_3.D_2O$ at 100 K. *J. Chem. Phys., 83,* 1449–1456.

Binet L., Gourier D., Derenne S., and Robert F. (2002) Heterogeneous distribution of paramagnetic radicals in insoluble organic matter from the Orgueil and Murchison meteorites. *Geochim. Cosmochim. Acta, 66,* 4177–4186.

Binet, L., Gourier D., Derenne S., Robert F., and Ciofini I. (2004) Occurence of abundant diradicaloid moieties in the insoluble organic matter from the Orgueil and Murchison meteorites: A fingerprint of its extraterrestrial origin? *Geochim. Cosmochim. Acta, 68,* 881–891.

Bishop J. L., Pieters C. M., and Burns R. G. (1993) Reflectance and Mössbauer spectroscopy of ferrihydrite-montmorillonite as Mars soil analog materials. *Geochim. Cosmochim. Acta, 57,* 4583–4595.

Bishop J., Madejova J., Komadel P., and Fröschl H. (2002a) The influence of structural Fe, Al and Mg on the infrared OH bands in spectra of dioctahedral smectites. *Clay Minerals, 37,* 607–616.

Bishop J., Murad E., and Dyar M. D. (2002b) The influence of octahedral and tetrahedral cation substitution on the structure of smectites and serpentines as observed through infrared spectroscopy. *Clay Minerals, 37,* 617–628.

Bohn R. B., Sandford S. A., Allamandola L. J., and Cruikshank D. P. (1994) Infrared spectroscopy of Triton and Pluto ice analogs: The case for saturated hydrocarbons. *Icarus, 111,* 151–173.

Bonal L., Quirico E., Bourot-Denise M., and Montagnac G. (2006) Determination of the petrologic type of CV3 chondrites by Raman spectroscopy of included organic matter. *Geochim. Cosmochim. Acta, 70,* 1849–1863.

Britt D. T., Bell J. F., Haack H., and Scott E. R. D. (1992) The reflectance spectrum of troilite (abstract). In *Lunar and Planetary Science XXIII,* pp. 167–168. Lunar and Planetary Institute, Houston.

Brown R. H. and Cruikshank D. P. (1997) Determination of the composition and state of icy surfaces in the outer solar system. *Annu. Rev. Earth Planet. Sci., 25,* 243–277.

Brown R. H., Cruikshank D. P., Tokunaga A. T., Smith R. G., and Clark R. N. (1988) Search for volatiles on icy satellites. I. — Europa. *Icarus, 74,* 262–271.

Brownlee D. E., Joswiak D. J., Bradley J. P., Gezo J. C., and Hill H. G. M. (2000) Spatially resolved acid dissolution of IDPs: The state of carbon and the abundance of diamonds in the dust (abstract). In *Lunar and Planetary Science XXXI,* Abstract #1921. Lunar and Planetary Institute, Houston (CD-ROM).

Brownlee D. E., Tsou P., Aléon J., Alexander C. M. O'D., Araki T., Bajt S., Baratta G. A., Bastien R., Bland P., Bleuet P., et al. (2006) Comet 81P/Wild 2 under a microscope. *Science, 314,* 1711–1716.

Brucato J. R., Colangeli L., Mennella V., Palumbo P., and Bussoletti E. (1999) Mid-infrared spectral evolution of thermally annealed amorphous pyroxene. *Astron. Astrophys., 348,* 1012–1019.

Brucato J. R., Mennella V., Colangeli L., Rotundi A., and Palumbo P. (2002) Production and processing of silicates in laboratory and in space. *Planet. Space. Sci., 50,* 829–837.

Brucato J. R., Strazzulla G., Baratta G., and Colangeli L. (2004) Forsterite amorphisation by ion irradiation: Monitoring by infrared spectroscopy. *Astron. Astrophys., 413,* 395–401.

Brunetto R., Baratta G. A., Domingo M., and Strazzulla G. (2005) Reflectance and transmittance spectra (2.2–2.4 μm) of ion irradiated frozen methanol. *Icarus, 175,* 226–232.

Burns R. G. (1970) *Mineralogical Applications to Crystal Field Theory.* Cambridge Univ., New York.

Calvin W. M. (1990) Additions and corrections to the absorption coefficients of CO_2 ice: Applications to the martian south polar cap. *J. Geophys. Res. (B), 95,* 14743–14750.

Calvin W. M., King T. V. V., and Clark R. N. (1994) Hydrous carbonates on Mars? Evidence from Mariner 6/7 infrared spectrometer and ground-based telescopic spectra. *J. Geophys. Res. (E), 99,* 14659–14675.

Chihara H., Koike C., Tsuchiyama A., Tachibana S., and Sakamoto D. (2002) Compositional dependence of infrared absorption spectra of crystalline silicates. I. Mg-Fe pyroxenes. *Astron. Astrophys., 391,* 267–273.

Christensen P. R., Bandfield J. L., Hamilton V. E., Howard D. A, Lane M. D., Piatek J. L., Ruff S. W., and Stefanov W. L. (2000) A thermal emission spectral library of rock-forming minerals. *J. Geophys. Res. (E), 105,* 9735–9740.

Clark R. N. and Roush T. L. (1984) Reflectance spectroscopy: Quantitative analysis techniques for remote sensing applications. *J. Geophys. Res., 89,* 6329–6340.

Clark R. N., Swayze G. A., Gallagher A. J., King T. V. V., and Calvin W. M (1993) *The U.S. Geological Survey, Digital Spectral Library: Version 1: 0.2 to 3.0 microns.* U.S. Geological Survey Open File Report 93–592, 1340 pp. Available online at *http://speclab.cr.usgs.gov*.

Cloutis E. A. (2003) Quantitative characterization of coal properties using bidirectional diffuse reflectance spectroscopy. *Fuel, 82,* 2239–2254.

Cloutis E. A. and Gaffey M. J. (1991) Pyroxene spectroscopy revisited: Spectral-compositional correlations and relationship to geothermometry. *J. Geophys. Res., 96,* 22809–22826.

Cloutis E. A. and Gaffey M. J. (1993) Accessory phases in aubrites: Spectral properties and implications for asteroid 44 Nysa. *Earth Moon Planets, 63,* 227–243.

Cloutis E. A., Gaffey M. J., Smith D. G. W., and Lambert R. St. J. (1990) Reflectance spectra of 'featureless' materials and the surface mineralogies of M- and E-class asteroids. *J. Geophys. Res., 95,* 281–293.

Cloutis E. A., Gaffey M. J., and Moslow T. F. (1994) Spectral reflectance properties of carbon-bearing materials. *Icarus, 107,* 276–287.

Cloutis E. A., Hawthorne F. C., Mertzman S. A., Krenn K., Craig M. A., Marcino D., Methot M., Strong J., Mustard J. F., Blaney D. L., Bell J. F. III, and Vilas F. (2006) Detection and discrimination of sulfate minerals using reflectance spectroscopy. *Icarus, 184,* 121–157.

Cody G. D. and Alexander C. M. O'D. (2005) NMR studies of chemical structural variation of insoluble organic matter from different carbonaceous chondrite groups. *Geochim. Cosmochim. Acta, 69,* 1085–1097.

Cody G. D., Alexander C. M. O'D., and Tera F. (2002) Solid-state (^{1}H and ^{13}C) nuclear magnetic resonance spectroscopy of insoluble organic residue in the Murchison meteorite: A self-consistent quantitative analysis. *Geochim. Cosmochim. Acta, 66,* 1851–1865.

Coll P., Coscia D., Smith N., Gazeau M.-C., Ramirez S. I., Cernogora G., Israel G., and Raulin F. (1999) Experimental laboratory simulation of Titan's atmosphere: Aerosols and gas phase. *Planet. Space Sci., 47,* 1331–1340.

Compagnini G. (1994) Optical constants of hydrogenated and unhydrogenated amorphous carbon in the 0.5–12 eV range. *Appl. Opt., 33,* 7377–7381.

Curchin J., Clark R. N., and Hoefen T. M. (2006) Cryogenic infrared reflectance spectra of organic ices and their relevance to the surface composition of Titan (abstract). *Bull. Am. Astron. Soc., 38,* 586–587.

Cruikshank D. P., Allamandola L. J., Hartmann W. K., Tholen D. J., Brown R. H., Matthews C. N., and Bell J. F. (1991) Solid CN bearing material on outer solar system bodies. *Icarus, 94,* 345–353.

Cruikshank D. P., Imanaka H., and Dalle Ore C. M. (1995) Tholins as coloring agents on outer solar system bodies. *Adv. Space Res., 36,* 178–183.

Cruikshank D. P., Roush T. L., Bartholomew M. J., Geballe T. R., Pendleton Y. J., White S. M., Bell J. F., Davies J. K., Owen T. C., de Bergh C., and 5 colleagues (1998) The composition of Centaur 5145 Pholus. *Icarus, 135,* 389–407.

Cruikshank D. P., Schmitt B., Roush T. L., Owen T. C., Quirico E., Geballe T. R., de Bergh C., Bartholomew M. J., Dalle Ore C., Douté S., and Meier R. (2000) Water ice on Triton. *Icarus, 147,* 309–316.

Cruikshank D. P., Dalle Ore C. M., Roush T. L., Geballe T. R., Owen T. C., de Bergh C., Cash M. D., Hartmann W. K., et al. (2001) Constraints on the composition of Trojan asteroid 624 Hektor. *Icarus, 153,* 348–360.

Cruikshank D. P., Owen T. C., Dalle Ore C., Geballe T. R., Roush T. L., de Bergh C., Sandford S. A., Poulet F., Benedix G. K., and Emery J. P. (2005a) A spectroscopic study of the surfaces of Saturn's large satellites: H_2O ice, tholins, and minor constituents. *Icarus, 175,* 268–283.

Cruikshank D. P., Imanaka H., and Dalle Ore C. M. (2005b) Tholins as coloring agents on outer solar system bodies. *Adv. Space Res., 36,* 178–183.

Dai Z. R. and Bradley J. P. (2005) Origin and properties of GEMS (glass with embedded metal and sulfides). In *Chondrites and the Protoplanetary Disk* (A. N. Krot et al., eds.), pp. 774–808. ASP Conf. Series 341, San Francisco.

Dartois E., Munoz Caro G. M., Deboffle D., Montagnac G., and d'Hendecourt L. (2005) Ultraviolet photoproduction of ISM dust. Laboratory characterisation and astrophysical relevance. *Astron. Astrophys., 432,* 895–908.

Day K. L. (1979) Mid-infrared optical properties of vapor-condensed magnesium silicates. *Astrophys. J., 234,* 158–161.

Day K. L. (1981) Infrared extinction of amorphous iron silicates. *Astrophys. J., 246,* 110–112.

Dello Russo N. and Khanna R. K. (1996) Laboratory infrared spectroscopic studies of crystalline nitriles with relevance to outer planetary systems. *Icarus, 123,* 366–395.

D'Hendecourt L. B.. and Allamandola L. J. (1986) Time dependent chemistry in dense molecular clouds. III. Infrared band cross sections of molecules in the solid state at 10 K. *Astron. Astrophys. Suppl. Ser., 64,* 453–467.

Dorschner J., Begemann B., Henning T., Jäger C., and Mutschke H. (1995) Steps toward interstellar silicate mineralogy. II. Study of Mg-Fe-silicate glasses of variable composition. *Astron. Astrophys., 300,* 503–520.

Douté S., Schmitt B., Quirico E., Owen T. C., Cruikshank D. P., de Bergh C., Geballe T. R., and Roush T. L. (1999) Evidence for methane segregation at the surface of Pluto. *Icarus, 142,* 421–444.

Douté S., Schmitt B., Langevin Y., Bibring J.-P., Altieri F., Bellucci G., Gondet B., Poulet F., and the MEX Team (2007) South pole of Mars: Nature and composition of the icy terrains from Mars Express OMEGA observations. *Planet. Space Sci., 55,* 113–133.

Durand B. (1980) Sedimentary organic matter and kerogen. Definition and qualitative importance of kerogen. In *Kerogen — Insoluble Organic Matter from Sedimentary Rocks* (B. Durand, ed.), pp. 13–34. Editions Technip, Paris.

Egan G. W. and Hilgeman T. (1977) The rings of Saturn — A frost-coated semiconductor. *Icarus, 30,* 413–421.

Ehrenfreund P., Robert F., D'Hendencourt L., and Behar F. (1991) Comparison of interstellar and meteoritic organic matter at 3.4 microns. *Astron. Astrophys., 252,* 712–717.

Emery J. P., Cruikshank D. P., and van Cleve J. (2006) Thermal emission spectroscopy (5.2–38 μm) of three Trojan asteroids with the Spitzer Space Telescope: Detection of fine-grained silicates. *Icarus, 182,* 496–512.

Espitalié J., Durand B., Roussel J. C., and Souron C. (1973) Etude de la matière organique insoluble (kérogène) des argiles du Toarcien du bassin de Paris. *Rev. Inst. Franç. du Pétrole, 28,* 37–66.

Fabian D., Jäger C., Henning Th., Dorschner J., and Mutschke H. (2000) Steps toward interstellar silicate mineralogy. V. Thermal evolution of amorphous magnesium silicates and silica. *Astron. Astrophys., 364,* 282–292.

Fabian D., Henning Th., Jäger C., Mutschke H., Dorschner J., and Wehrhan O. (2001) Steps toward interstellar silicate mineralogy. VI. Dependence of crystalline olivine IR spectra on iron content and particle shape. *Astron. Astrophys., 378,* 228–238.

Ferrari A. C. and Robertson J. (2000) Interpretation of Raman spectra of disordered and amorphous carbon. *Phys. Rev. B, 61,* 14095–14107.

Ferrari A. C., Rodil S. E., and Robertson J. (2003) Interpretation of infrared and Raman spectra of amorphous carbon nitrides. *Phys. Rev. B, 67,* 155306.

Ferris J., Tran B., Joseph J., Vuitton V., Briggs R., and Force M. (2005) The role of photochemistry in Titan's atmospheric chemistry. *Adv. Space Res., 36,* 251–257.

Fink U. and Sill G. T. (1982) The infrared spectral properties of frozen volatiles. In *Comets* (L. L. Wilkening, ed.), pp. 164–202. Univ. of Arizona, Tucson.

Flynn G. J., Keller L. P., Feser M., Wirick S., and Jacobsen C. (2003) The origin of organic matter in the solar system: Evidence from the interplanetary dust particles. *Geochim. Cosmochim. Acta, 67,* 4791–4806.

Flynn G. J., Keller L. P., Jacobsen C., and Wirick S. (2004) An assessment of the amount and types of organic matter contributed to the Earth by interplanetary dust. *Adv. Space Res., 33,* 57–66.

Forrest W. J., Houck J. R., and McCarthy J. F. (1981) A far-infrared emission feature in carbon-rich stars and planetary nebulae. *Astrophys. J., 248,* 195–200.

Foster P. J. and Howarth C. R. (1968) Optical constants of carbons and coals in the infrared. *Carbon, 6,* 719–729.

Gaffey M. J. (1976) Spectral reflectance characteristics of the meteorite classes. *J. Geophys. Res., 81,* 905–920.

Ganz H. and Kalkreuth W. (1987) Application of infrared spectroscopy to the classification of kerogen-types and the evaluation of source rock and oil shale potentials. *Fuel, 66,* 708–711.

Gardinier A., Derenne S., Robert F., Behar F., Largeau C., and Maquet J. (2000) Solid state CP/MAS ^{13}C NMR of the insoluble organic matter of the Orgueil and Murchison meteorites: Quantitative study. *Earth Planet. Sci. Lett., 184,* 9–21.

Gerakines P. A., Bray J. J., Davis A., and Richey C. R. (2005) The strengths of near-infrared absorption features relevant to interstellar and planetary ices. *Astrophys. J., 620,* 1140–1150.

Goodman M. A., Sweany R. L., and Flurry R. L. Jr. (1983) Infrared spectra of matrix-isolated, crystalline solid, and gas phase C_3-C_6 n-alkanes. *J. Phys. Chem., 87,* 1753–1757.

Green J. R., Brown R. H., Cruikshank D. P., and Anicich V. (1991) The absorption coefficient of nitrogen with application to Triton (abstract). *Bull. Am. Astron. Soc., 23,* 1208.

Grundy W. M. and Schmitt B. (1998) The temperature-dependent near-infrared absorption spectrum of hexagonal H_2O ice. *J. Geophys. Res. (E), 103,* 25809–25822.

Grundy W. M., Schmitt B., and Quirico E. (1993) The temperature dependent spectra of α and β nitrogen ice with application to Triton. *Icarus, 105,* 254–258.

Grundy W. M., Schmitt B., and Quirico E. (2002) The temperature-dependent spectrum of methane ice I between 0.7 and 5 μm and opportunities for near-infrared thermometry. *Icarus, 155,* 486–496.

Guillois O., Nenner I., Papoular R., and Reynaud C. (1996) Coal models for the infrared emission spectra of proto-planetary nebulae. *Astrophys. J., 464,* 810–817.

Halbout J., Robert F., and Javoy M. (1990) Hydrogen and oxygen isotope compositions in kerogen from the Orgueil meteorite — Clues to a solar origin. *Geochim. Cosmochim. Acta, 54,* 1453–1462.

Hansen G. B. (1996) The infrared absorption spectrum of carbon dioxide ice. Ph.D. thesis, Univ. of Washington.

Hansen G. B. (1997) The infrared absorption spectrum of carbon dioxide ice from 1.8 to 333 μm. *J. Geophys. Res. (E), 102,* 21569–21588.

Hansen G. B. (2005) Ultraviolet to near-infrared absorption spectrum of carbon dioxide ice from 0.174 to 1.8 μm. *J. Geophys. Res. (E), 110,* E11003.

Hapke B. (2001) Space weathering from Mercury to the asteroid belt. *J. Geophys. Res. (E), 106,* 10039–10074.

Hapke B. and Wells E. (1981) Bidirectional reflectance spectroscopy. 2. Experiments and observations. *J. Geophys. Res., 96,* 3055–3060.

Harvey K. B. and Ogilvie J. F. (1962) Infrared absorption of formaldehyde at low temperatures: Evidence for multiple trapping sites in an argon matrix. *Can. J. Chem., 40,* 85–91.

Hayatsu R. and Anders E. (1981) Organic compounds in meteorites and their origins. *Topics in Current Chemistry, 99,* 1–37.

Hayatsu R., Matsuoka S., Anders E., Scott R. G., and Studier M. H. (1977) Origin of organic matter in the early solar system. VII — The organic polymer in carbonaceous chondrites. *Geochim. Cosmochim. Acta, 41,* 1325–1339.

Hayatsu R., Scott R. G., and Winans R. E. (1983) Comparative structural study of meteoritic polymer with terrestrial geopolymers coal and kerogen. *Meteoritics, 18,* 310.

Henning Th. and Mutschke H. (1997) Low-temperature infrared properties of cosmic dust analogues. *Astron. Astrophys., 327,* 743–754.

Henning Th., Il'in V. B., Krivova N. A., Michel B., and Voshchinnikov N. V. (1999) WWW database of optical constants for astronomy. *Astron. Astrophys. Suppl. Ser., 136,* 405–406.

Hinrichs J. L. and Lucey P. G. (2002) Temperature-dependent near-infrared spectral properties of minerals, meteorites, and lunar soil. *Icarus, 155,* 169–180.

Hony S., Bouwman J., Keller L. P., and Waters L. B. F. M. (2002) The detection of iron sulfides in planetary nebulae. *Astron. Astrophys., 393,* L103–L106.

Hudgins D. M., Sandford S. A., Allamandola L. J., and Tielens A. G. G. M. (1993) Mid- and far-infrared spectroscopy of ices: Optical constants and integrated absorbances. *Astrophys. J. Suppl. Ser., 86,* 713–870.

Hudson R. L. and Moore M. H. (1993) Far-infrared investigations of a methanol clathrate hydrate — Implications for astronomical observations. *Astrophys. J., 404,* L29–L32.

Huffman D. R. (1975) Optical properties of particulates. *Astrophys. Space Sci., 34,* 175–184.

Huffman D. R. and Stapp J. L. (1973) Optical measurements on solids of possible interstellar importance. In *Interstellar Dust and Related Topic*s (J. M. Greenberg and H. van der Hulst, eds.), pp. 297–302. IAU Symposium No. 52, Reidel, Dordrecht.

Huss G. R., Meshik A. P., Smith J. B., and Hohenberg C. M. (2003) Presolar diamond, silicon carbide, and graphite in carbonaceous chondrites: Implications for thermal processing in the solar nebula. *Geochim. Cosmochim. Acta, 67,* 4823–4848.

Iglesias-Groth S. (2004) Fullerenes and buckyonions in the interstellar medium. *Astrophys. J. Lett., 608,* L37–L40.

Imanaka H., Khare B. N., Elsila J. E., Bakes E. L. O., McKay C. P., Cruikshank D. P., Sugita S., Matsui T., and Zare R. N. (2004) Laboratory experiments of Titan tholin formed in cold plasma at various pressures: Implications for nitrogen-containing polycyclic aromatic compounds in Titan haze. *Icarus, 168,* 344–366.

Jäger C., Mutschke H., and Henning Th. (1998a) Optical proper-

ties of carbonaceous dust analogues. *Astron. Astrophys., 332,* 291–299.

Jäger C., Molster F. J., Dorschner J., Henning Th., Mutschke H., and Waters L. B. F. M. (1998b) Steps toward interstellar silicate mineralogy. IV. The crystalline revolution. *Astron. Astrophys., 339,* 904–916.

Jessberger E. K., Christoforidis A., and Kissel J. (1988) Aspects of the major element composition of Halley's dust. *Nature, 332,* 691–695.

Keller L. P., Thomas K. L., and McKay D. S. (1994) Carbon in primitive interplanetary dust particles. In *Analysis of Interplanetary Dust* (G. J. Flynn et al., eds.), pp. 159–164. AIP Conf. Proc. 310, American Institute of Physics, New York.

Keller L. P., Hony S., Bradley J. P., Molster F. J., Waters L. B. F. M., Bouwman J., de Koter A., Brownlee D. E., Flynn G. J., Henning Th., and Mutschke H. (2002) Identification of iron sulphide grains in protoplanetary disks. *Nature, 417,* 148–150.

Keller L. P., Bajt S., Baratta G., Borg J., Bradley J. P., Brownlee D. E., Busemann H., Brucato J. R., Burchell M., Colangeli L., et al. (2006) Infrared spectroscopy of Comet 81P/Wild 2 samples returned by Stardust. *Science, 314,* 1728–1731.

Kerridge J. F. (1999) Formation and processing of organics in the early solar system. *Space Sci. Rev., 90,* 275–288.

Khanna R. K., Ospina M. J., and Zhao G. (1988) Infrared band extinctions and complex refractive indices of crystalline C_2H_2 and C_4H_2. *Icarus, 74,* 527–535.

Khare B. N., Sagan C., Arakawa E. T., Suits F., Callcott T. A., and Williams M. W. (1984) Optical constants of organic tholins produced in a simulated titanian atmosphere: From soft X-ray to microwave frequencies. *Icarus, 60,* 127–137.

Khare B. N., Sagan C., Thompson W. R., Arakawa E. T., and Votaw P. (1987) Solid hydrocarbon aerosols produced in simulated Uranian and Neptunian stratospheres. *J. Geophys. Res., 92,* 15067–15082.

Khare B. N., Thompson W. R., Sagan C., Arakawa E. T., Bruel C., Judish J. P., Khanna R. K., and Pollack J. B. (1990a) Optical constants of solid methane. In *First International Conference on Laboratory Research of Planetary Atmospheres* (K. Fox et al., eds.), pp. 327–339. NASA CP-3077, Washington, DC.

Khare B. N., Thompson W. R., Sagan C., Arakawa E. T., Meisse C., and Gilmour I. (1990b) Optical constants of kerogen from 0.15 to 40 μm: Comparison with meteoritic organics. In *First International Conf. on Laboratory Research for Planetary Atmospheres* (K. Fox et al., eds.), p. 340. NASA CP-3077, Washington, DC.

Khare B. N., Thompson W. R., Cheng L., Chyba C., and Sagan C. (1993) Production and optical constants of ice tholin from charged particule irradiation of (1:6) C_2H_6/H_2O at 77 K. *Icarus, 103,* 290–300.

Khare B. N., Sagan C., Thompson W. R., Arakawa E. T., Meisse C., and Tuminello P. S. (1994) Optical properties of poly-HCN and their astronomical applications. *Can. J. Chem., 72,* 678–694.

Khare B. N., Bakes E. L. O., Imanaka H., McKay C. P., Cruikshank D. P., and Arakawa E. T. (2002) Analysis of the time-dependent chemical evolution of Titan haze tholin. *Icarus, 160,* 172–182.

Kimura Y., Tamura K., Koike C., Chihara H., and Kaito C. (2005) Laboratory production of monophase pyrrhotite grains using solid-solid reaction and their characteristic infrared spectra. *Icarus, 177,* 280–285.

King T. V. V. and Ridley W. I. (1987) Relation of the spectroscopic reflectance of olivine to mineral chemistry and some remote sensing implications. *J. Geophys. Res., 92,* 11457–11469.

Kissel J. and Krueger F. R. (1987) The organic component in dust from Comet Halley as measured by the PUMA mass spectrometer on board Vega 1. *Nature, 326,* 755–760.

Knief S. and von Niessen W. (1999) Disorder, defects, and optical absorption in a-Si and a-Si:H. *Phys. Rev. B, 59,* 12940–12946.

Koike C. and Tsuchiyama A. (1992) Simulation and alteration for amorphous silicates with very broad bands in infrared spectra. *Mon. Not. R. Astron. Soc., 255,* 248–254.

Koike C., Chihara H., Tsuchiyama A., Suto H., Sogawa H., and Okuda H. (2003) Compositional dependence of infrared absorption spectra of crystalline silicate. II. Natural and synthetic olivines. *Astron. Astrophys., 399,* 1101–1107.

Koike C., Mutschke H., Suto H., Naoi T., Chihara H., Henning Th., Jäger C., Tsuchiyama A., Dorschner J., and Okuda H. (2006) Temperature effects on the mid-and far-infrared spectra of olivine particles. *Astron. Astrophys., 449,* 583–596.

Krasnopolsky V. A. and Cruikshank D. P. (1999) Photochemistry of Pluto's atmosphere and ionosphere near perihelion. *J. Geophys. Res., 104,* 21979–21996.

Lisse C. M., VanCleve J., Adams A. C., A'Hearn M. F., Fernández Y. R., Farnham T. L., Armus L., Grillmair C. J., Ingalls J., Belton M. J. S., et al. (2006) Spitzer spectral observations of the Deep Impact ejecta. *Science, 313,* 635–640.

Logan L. and Hunt G. R. (1970) Emission spectra of particulate silicates under simulated lunar conditions. *J. Geophys. Res., 75,* 6539–6548.

Logothetidis S., Petalas J., and Ves S. (1995) The optical properties of a-C:H films between 1.5 and 10 eV and the effect of thermal annealing on the film character. *J. Appl. Phys., 79,* 1040–1050.

Lucey P. G. (1998) Model near-infrared optical constants of olivine and pyroxene as a function of iron content. *J. Geophys. Res. (E), 103,* 1703–1713.

Lyon R. J. P. (1964) Analysis of rocks by spectral infrared emission (8 to 25 microns). *Econ. Geol., 60,* 717–736.

Martonchik J. V., Orton G. S., and Appleby J. F. (1984) Optical properties of NH_3 ice from the far infrared to the near ultraviolet. *Appl. Opt., 23,* 541–547.

Masterson C. M. and Khanna R. K. (1990) Absorption intensities and complex refractive indices of crystalline HCN, HC_3N, and C_4N_2 in the infrared region. *Icarus, 83,* 83–92.

Mastrapa R. M. E. and Brown R. H. (2006) Ion irradiation of crystalline H_2O-ice: Effect on the 1.65-μm band. *Icarus, 183,* 207–214.

Maturilli A., Helbert J., and Moroz L. V. (2007) The Berlin Emissivity Database (BED). *Planet. Space Sci.,* in press.

McDonald G. D., Khare B. N., Thompson W. R., and Sagan C. (1991) $CH_4/NH_3/H_2O$ spark tholin: Chemical analysis and interaction with jovian aqueous clouds. *Icarus, 94,* 354–367.

McDonald G. D., Thompson W. R., Heinrich M., Khare B. N., and Sagan C. (1994) Chemical investigation of Titan and Triton tholins. *Icarus, 108,* 137–145.

McDonald G. D., Whited L. J., DeRuiter C., Khare B. N., Patnaik A., and Sagan C. (1996) Production and chemical analysis of cometary ice tholins. *Icarus, 122,* 107–117.

McKay C. O. (1996) Elemental composition, solubility, and optical properties of Titan's organic haze. *Planet. Space Sci., 44,* 741–747.

Minard R. D., Hatcher P. G., and Gourley R. C. (1998) Structural investigations of hydrogen cyanide polymers: New insights using TMAH thermochemolysis/GC-MS. *Origins Evol. Biosph., 28,* 461–473.

Moore M. H. and Hudson R. L. (1992) Far-infrared spectral studies of phase changes in water ice induced by proton irradiation. *Astrophys. J., 401,* 353–360.

Moore M. H., Ferrante R. F., Hudson R. L., Nuth J. A. III, and Donn B. (1994) Infrared spectra of crystalline phase ices condensed on silicate smokes at T < 20 K. *Astrophys. J. Lett., 428,* L81–L84.

Moore M. H., Ferrante R. F., Hudson R. L., and Stone J. N. (2007) Ammonia-water ice laboratory studies relevant to outer solar system surfaces. *Icarus, 190,* 260–273.

Moroz L. V., Pieters C. M., and Akhmanova M. V. (1992) Why the surfaces of outer belt asteroids are dark and red? (abstract). In *Lunar and Planetary Science XXIII,* pp. 931–932. Lunar and Planetary Institute, Houston.

Moroz L. V., Arnold G., Korochantsev A., and Wäsch R. (1998) Natural solid bitumens as possible analogs for cometary and asteroid organics: 1. Reflectance spectroscopy of pure bitumens. *Icarus, 134,* 253–268.

Moroz L. V., Schade U., and Wäsch R. (2000) Reflectance spectra of olivine-orthopyroxene-bearing assemblages at decreased temperatures: Implications for remote sensing of asteroids. *Icarus, 147,* 79–93.

Moroz L. V., Schmidt M., Schade U., Hiroi T., and Ivanova M. A. (2006) Synchrotron-based IR microspectroscopy as a useful tool to study hydration states of meteorite constituents. *Meteoritics & Planet. Sci., 41,* 1219–1230.

Mukai T. and Krätschmer W. (1986) Optical constants of the mixture of ices. *Earth Moon Planets, 36,* 145–155.

Mukai T. and Koike C. (1990) Optical constants of olivine particles between wavelengths of 7 and 200 microns. *Icarus, 87,* 180–187.

Murae T. (1994) FT-IR spectroscopic studies of major organic matter in carbonaceous chondrites using microscopic technique and comparison with terrestrial kerogen. *Proc. NIPR Symp. Antarct. Meteorites, 7,* 262–274.

Murae T., Masuda A., and Takahashi T. (1990) Spectroscopic studies of acid-resistant residues of carbonaceous chondrites. *Proc. NIPR Symp. Antarct. Meteorites, 3,* 211–219.

Mustard J. F. and Hays J. E. (1997) Effects of hyperfine particles on reflectance spectra from 0.3 to 25 μm. *Icarus, 125,* 145–163.

Mutsukura N. and Akita K-I. (1999) Infrared absorption spectroscopy measurements of amorphous CNx films prepared in CH_4/N_2 r.f. discharge. *Thin Solid Films, 349,* 115–119.

Nelander B. (1976) On the infrared spectrum of a carbon dioxide containing nitrogen matrix. *Chem. Phys. Lett., 42,* 187–189.

Ospina M., Zhao G., and Khanna R. K. (1988) Absolute intensities and optical constants of crystalline C_2N_2 in the infrared region. *Spectrochim. Acta A, 44,* 23–26.

Ossenkopf V., Henning Th., and Mathis J. S. (1992) Constraints on cosmic silicates. *Astron. Astrophys., 261,* 567–578.

Painter P., Starsinic M., and Coleman M. (1985) Determination of functional groups in coal by fourier transform interferometry. In *Fourier Transform Infrared Spectroscopy: Vol. 4, Application to Chemical Systems* (J. R. Ferraro and L. J.Basile, eds.), pp. 169–241. Academic, London.

Palumbo M. E. and Strazzulla G. (2003) Nitrogen condensation on water ice. *Can. J. Phys., 81,* 217–224.

Papoular R. (2001) The use of kerogen data in understanding the properties and evolution of interstellar carbonaceous dust. *Astron. Astrophys., 378,* 597–607.

Papoular R., Reynaud C., and Nenner I. (1991) The coal model for the unidentified infrared bands. II — The thermal emission mechanism. *Astron. Astrophys., 247,* 215–225.

Papoular R., Breton J., Gensterblum G., Nenner I., Papoular R. J., and Pireaux J.-J. (1993) The vis/UV spectrum of coals and the interstellar extinction curve. *Astron. Astrophys., 270,* L5–L8.

Pearl J., Ngoh M., Ospina M., and Khanna R. (1991) Optical constants of solid methane and ethane from 10000 to 450 cm^{-1}. *J. Geophys. Res., 96,* 17477–17482.

Pendleton Y. (1995) Laboratory comparisons of organic materials to interstellar dust and the Murchison meteorite. *Planet. Space Sci., 43,* 1359–1364.

Pendleton Y. J. and Allamandola L. J. (2002) The organic refractory material in the diffuse interstellar medium: Mid-infrared spectroscopic constraints. *Astrophys. J. Suppl. Ser., 138,* 75–98.

Pieters C. M. and Hiroi T. (2004) RELAB (Reflectance Experiment Laboratory): A NASA Multiuser Spectroscopy Facility (abstract). In *Lunar and Planetary Science XXXV,* Abstract #1720. Lunar and Planetary Institute, Houston (CD-ROM).

Pizzarello S., Huang Y., Becker L., Poreda R. J., Nieman R. A., Cooper G., and Williams M. (2001) The organic content of the Tagish Lake meteorite. *Science, 293,* 2236–2239.

Pollack J. B., Hollenbach D., Beckwith S., Simonelli D. P., Roush T. L., and Fong W. (1994) Composition and radiative properties of grains in molecular clouds and accretion disks. *Astrophys. J., 421,* 615–639.

Preibisch Th., Ossenkopf V., Yorke H.W., and Henning Th. (1993) The influence of ice-coated grains on protostellar spectra. *Astron. Astrophys., 279,* 577–588.

Quirico E. and Schmitt B. (1997a) Near-infrared spectroscopy of simple hydrocarbons and carbon oxides diluted in solid N_2 and as pure ices: Implications for Triton and Pluto. *Icarus, 127,* 354–378.

Quirico E. and Schmitt B. (1997b) A spectroscopic study of CO diluted in N_2 ice: Applications for Triton and Pluto. *Icarus, 128,* 181–188.

Quirico E., Schmitt B., Bini R., and Salvi P. R. (1996) Spectroscopy of some ices of astrophysical interest: SO_2, N_2 and N_2:CH_4 mixtures. *Planet. Space Sci., 44,* 973–986.

Quirico E., Douté S., Schmitt B., de Bergh C., Cruikshank D. P., Owen T. C., Geballe T. R., and Roush T.L. (1999) Composition, physical state and distribution of ices at the surface of Triton. *Icarus, 139,* 159–178.

Quirico E., Raynal P. I., and Bourot-Denise M. (2003) Metamorphic grade of organic matter in six unequilibrated ordinary chondrites. *Meteoritics & Planet. Sci., 38,* 795–811.

Quirico E., Borg J. Raynal P-Y., Montagnac G., and d'Hendecourt L. (2005) A micro-Raman survey of 10 IDPs and 6 carbonaceous chondrites. *Planet. Space Sci., 53,* 1443–1448.

Quirico E., Bernard J.-M., Montagnac G., Rouzaud J.-N., Szopa C., Cernogora G., Reynard B., McMillan P., Fray N., Schmitt B., Coll P., and Raulin F. (2006) Chemical structure and optical properties of Titan's tholins and HCN polymer. Implications for the analysis of Cassini-Huygens observations and refractory organics in cometary grains (abstract). In *Lunar and Planetary Science XXXVII,* Abstract #2105. Lunar and Planetary Institute, Houston (CD-ROM).

Ramirez S. I., Coll P., da Silva A., Navarro-Gonzalez R., Lafait J., and Raulin F. (2002) Complex refractive index of Titan's aerosol analogues in the 200–900 nm domain. *Icarus, 156,* 515–529.

Robert F. and Epstein S. (1982) The concentration and isotopic composition of hydrogen, carbon and nitrogen in carbonaceous

meteorites. *Geochim. Cosmochim. Acta, 46,* 81–95.

Robin P. L. and Rouxhet P. G. (1976) Contribution des différentes fonctions chimiques dans les bandes d'absorption infrarouge des kérogènes situées à 1710, 1630 et 3430 cm^{-1}. *Rev. Inst. Franç. du Pétrole, 31,* 955–978.

Rodil S. E., Ferrari A. C., Robertson J., and Milne W. I. (2001) Raman and infrared modes of hydrogenated amorphous carbon nitride. *J. Appl. Phys., 89,* 5425–5430.

Rodil S. E., Ferrari A. C., Robertson J., and Muhl S. (2003) Infrared spectra of carbon nitride films. *Thin Solid Films, 420,* 122–131.

Rouleau F. and Martin P. (1991) Shape and clustering effects on the optical properties of amorphous carbon. *Astrophys. J., 377,* 526–540.

Roush T. L. (1995) Optical constants of amorphous carbon in the mid-IR (2.5–25 μm, 4000–400 cm^{-1}). *Planet. Space Sci., 43,* 1297–1301.

Roush T. L. (2003) Estimated optical constants of the Tagish Lake meteorite. *Meteoritics & Planet. Sci., 38,* 419–426.

Roush T. L. and Dalton J. B. (1994) Reflectance spectra of hydrated Titan tholins at cryogenic temperatures and implications for compositional interpretation of red objects in the outer solar system. *Icarus, 168,* 158–162.

Roush T., Pollack J., and Orenberg J. (1991) Derivation of mid-infrared (5–25 microns) optical constants of some silicates and palagonite. *Icarus, 94,* 191–208.

Rouxhet P. G., Robin P. L., and Nicaise G. (1980) Characterization of kerogen and their evolution by infrared spectroscopy. In *Kerogen — Insoluble Organic Matter from Sedimentary Rocks* (B. Durand, ed.), pp. 13–34. Editions Technip, Paris.

Sagan C. and Khare B. N. (1979) Tholins: Organic chemistry of interstellar grains and gas. *Nature, 277,* 102–107.

Sagan C., Khare B. N., and Lewis J. S. (1984) Organic matter in the solar system. In *Saturn* (T. Gehrels and M. S. Matthews, eds.), pp. 788–807. Univ. of Arizona, Tucson.

Sandford S. A. (1996) The inventory of interstellar materials available for the formation of the solar system. *Meteoritics & Planet. Sci., 31,* 449–476.

Sandford S. A., Aléon J., Alexander C. M. O'D., Araki T., Bajt S., Baratta G. A., Borg J., Bradley J. P., Brownlee D. E., Brucato J. R., et al. (2006) Organics captured from Comet 81P/Wild 2 by the Stardust spacecraft. *Science, 314,* 1720–1724.

Satorre M. A., Palumbo M. E., and Strazzulla G. (2001) Infrared spectra of N_2 rich ice mixtures. *J. Geophys. Res. (E), 106,* 33363–33370.

Schmitt B., Grim R. J. A., and Greenberg J. M (1989) Spectroscopy and physico-chemistry of CO:H_2O and CO_2:H_2O ices. In *22nd ESLAB Symposium: Infrared Spectroscopy in Astronomy,* pp. 213–219. ESA Spec. Publ. 290, Noordwijk, The Netherlands.

Schmitt B., Oehler A., Calvier R., Haschberger P., and Lindermeier E. (1990) The near infrared absorption features of solid nitrogen and methane on Triton (abstract). *Bull. Am. Astron. Soc., 22,* 1121.

Schmitt B., Quirico E., and Lellouch E. (1992) Near infrared spectra of potential solids at the surface of Titan. In *Proceedings of the Symposium on Titan,* pp. 383–388. ESA Spec. Publ. 338, Noordwijk, The Netherlands.

Schmitt B., de Bergh C., Lellouch E., Maillard J. P., Barbe A., and Douté S. (1994) Identification of three absorption bands in the two micron spectrum of Io. *Icarus, 111,* 79–105.

Schmitt B., Quirico E., Trotta F., and Grundy W. (1998) Optical properties of ices from UV to infrared. In *Solar System Ices* (B. Schmitt et al., eds.), pp. 199–240. Astrophys. Space Sci. Lib. Vol. 227, Kluwer, Dordrecht.

Schnaiter M., Henning Th., Mutschke H., Kohn B., Ehbrecht M., and Huisken F. (1999) Infrared spectroscopy of nano-sized carbon grains produced by laser pyrolysis of acetylene: Analog materials for interstellar grains. *Astrophys. J., 519,* 687–696.

Schulze H., Kissel J., and Jessberger E. K. (1997) Chemistry and mineralogy of comet Halley's dust. In *From Stardust to Planetesimals* (Y. J. Pendleton and A. G. G. M. Tielens, eds.), pp. 397–414. ASP Conf. Series 122, San Francisco.

Scott A. and Duley W. W. (1996) Ultraviolet and infrared refractive indices of amorphous silicates. *Astrophys. J. Suppl. Ser., 105,* 401–405.

Shkuratov Y., Starukhina L., Hoffmann H., and Arnold G. (1999) A model of spectral albedo of particulate surfaces: Implications for optical properties of the Moon. *Icarus, 137,* 235–246.

Sill G. S., Fink U., and Ferraro J. R. (1980) Absorption coefficients of solid NH_3 from 50 to 7000 cm^{-1}. *J. Opt. Soc. Am., 70,* 724–739.

Singer R. B. and Roush T. L. (1985) Effects of temperature on remotely sensed mineral absorption features. *J. Geophys. Res., 90,* 12434–12444.

Smith R. G., Robinson G., Hyland A. R., and Carpenter G. L. (1994) Molecular ices as temperature indicators for insterstellar dust: The 44 and 62 μm lattice features of H_2O ice. *Mon. Not. R. Astron. Soc., 271,* 481–489.

Sourisseau C., Coddens G., and Papoular R. (1992) On the 21-micron feature of pre-planetary nebulae. *Astron. Astrophys., 254,* L1–L4.

Sunshine J. M. and Pieters C. M. (1998) Determining the composition of olivine from reflectance spectroscopy. *J. Geophys. Res. (E), 103,* 13675–13688.

Szopa C., Cernogora G., Boufendi L., Correia J. J., and Coll P. (2006) PAMPRE: A dusty plasma experiment for Titan's tholins production and study. *Planet. Space Sci., 54,* 394–404.

Taylor F. W. (1973) Preliminary data on the optical properties of solid ammonia and scattering parameters for ammonia cloud particles. *J. Atmos. Sci., 30,* 677–683.

Tielens A. G. G. M. (1997) Circumstellar PAHs and carbon stardust. *Astrophys. Space Sci., 251,* 1–13.

Toon O. B., Tolbert M. A., Koehler B. G., Middlebrook A. M., and Jordan J. (1994) Infrared optical constants of H_2O ice, amorphous nitric acid solutions, and nitric acid hydrates. *J. Geophys. Res. (D), 99,* 25631–25654.

Tran B. N., Joseph J. C., Ferris J. P., Persans P. D., and Chera J. J. (2003) Simulation of Titan haze formation using a photochemical flow reactor. The optical constants of the polymer. *Icarus, 165,* 379–390.

Trotta F. (1996) Détermination des constantes optiques de glaces dans l'infrarouge moyen et lointain. Application aux grains du milieu interstellaire et des enveloppes circumstellaires. Thesis, LGGE — Université Joseph Fourier, Grenoble, France.

Trotta F. and Schmitt B. (1996) Determination of the optical constants of solids in the mid infrared. In *The Cosmic Dust Connection* (J. M. Greenberg, ed.), pp. 179–184. NATO ASI Series C 487, Kluwer, Dordrecht.

Tryka K. A., Brown R. H., Anicich V., Cruikshank D. P., and Owen T. C. (1993) Spectroscopic determination of the phase composition and temperature of nitrogen ice on Triton. *Science, 261,* 751–754.

Tryka K. A., Brown R. H., and Anicich V. (1995) Near-infrared

absorption coefficients of solid nitrogen as a function of temperature. *Icarus, 116,* 409–414.

Van Krevelen D. W. (1961) Optical properties: Refractometric and spectrometric analysis of coal. In *Coal,* pp. 343–372. Elsevier, Amsterdam.

Warren S. G. (1984) Optical constants of ice from the ultraviolet to the microwave. *Appl. Opt., 23,* 1206–1223.

Warren S. G. (1986) Optical constants of carbon dioxide ice. *Appl. Opt., 25,* 2650–2674.

Wdowiak T. J., Flickinger G. C., and Cronin J. R. (1988) Insoluble organic material in Orgueil carbonaceous chondrite and the unidentified infrared bands. *Astrophys. J. Lett., 328,* L75–L79.

Wisnosky M. G., Eggers D. F., Fredrickson L. R., and Decius J. C. (1983) The vibrational spectra of solid II ethane and ethane-d_6. *J. Chem. Phys., 79,* 3505–3512.

Wooden D. H., Harker D. E., and Brearley A. J. (2005) Thermal processing and radial mixing of dust: Evidence from comets and primitive chondrites. In *Chondrites and the Protoplanetary Disk* (A. N. Krot et al., eds.), pp. 774–808. ASP Conf. Series 341, San Francisco.

Wopenka B. (1988) Raman observations on individual interplanetary dust particles. *Earth Planet. Sci. Lett., 88,* 221–231.

Wright I. P., McGarvie D. W., Grady M. M., and Pillinger C. T. (1990) The distribution of carbon in C1 to C6 carbonaceous chondrites. *Proc. NIPR. Symp. Antarct. Meteorites, 3,* 194–210.

Zolensky M. E. and Thomas K. L. (1995) Iron and iron-nickel sulfides in chondritic interplanetary dust particles. *Geochim. Cosmochim. Acta, 59,* 4707–4712.

Zolensky M. E., Zega T. J., Yano H.,Wirick S., Westphal A. J., Weisberg M. K., Weber I., Warren J. L., Velbel M. A., Tsuchiyama A., et al. (2006) Mineralogy and petrology of Comet 81P/Wild 2 nucleus samples. *Science, 314,* 1735–1739.

Zubko V., Mennella V., Colangeli L., and Bussoletti E. (1996) Optical constants of amorphous carbon grains. In *The Role of Dust in the Formation of Stars* (H. U. Käufl and R. Siebenmorgen, eds.), p. 333. ESO Astrophysics Symposia, European Southern Observatory/Springer-Verlag, Berlin.